

VIII CHAPTER: TRANSPORT PHENOMENA

VIII.1	Diffusion: Experimental methods	1
VIII.2	Electromigration: Experimental methods	20
VIII.3	Thermomigration	27
VIII.4	Thermodynamics of irreversible processes	30
	VIII.4.1 Diffusion	38
	VIII.4.2 Electromigration	40
	VIII.4.3 Thermomigration	42
VIII.5	References	43

One of the remarkable properties of hydrogen in metals is its fast diffusion. Around room temperature diffusion coefficients of the order of $10^{-5} \text{ cm}^2/\text{s}$ are not uncommon. This corresponds to approximately 2 mm per hour, which is indeed a very high value for diffusion in a solid. In this chapter we shall give a phenomenological description of diffusion, electromigration and thermomigration of interstitial atoms. In diffusion, the migration of atoms is produced by a concentration gradient, while in electromigration their displacement is caused by an applied electric field. In thermomigration the driving force is a temperature gradient over the sample.

We review first some experimental methods used to measure the migration of hydrogen and other interstitials.

VIII.1 DIFFUSION: EXPERIMENTAL METHODS

In almost all methods used to determine the diffusion of hydrogen in a metal one measures the time evolution of an initially inhomogeneous concentration distribution of hydrogen atoms. The most widely used methods are:

- Permeation methods (D1)
- Electrolytic methods (D2)
- The Gorsky effect (D3)
- Resistivity relaxation (D4)
- Nuclear magnetic resonance (D5)
- Quasi-elastic neutron diffraction (D6)
- Optical method (D7)

D1 Permeation methods

Hydrogen is forced through a thin membrane by a pressure difference, p_2 being larger than p_1 . From Fick's first law, the current density \mathbf{j} is given by

$$\mathbf{j} = -D \text{grad} c \quad \rightarrow \quad \mathbf{j} = D \frac{c_2 - c_1}{d} \quad (\text{VIII.1})$$

in a stationary state.

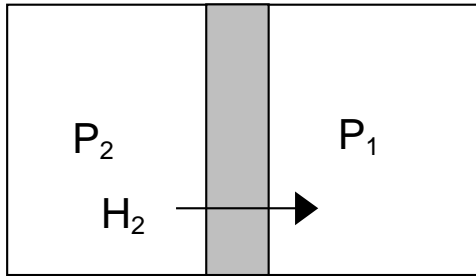


Fig. VIII.1: Configuration of a hydrogen permeation experiment. Hydrogen is forced through the membrane by the pressure difference $p_2 - p_1$.

From Sievert's law (see Eq.III.54)

$$c_i = K\sqrt{p_i} \quad (\text{VIII.2})$$

and thus

$$\mathbf{j} = DK \frac{\sqrt{p_2} - \sqrt{p_1}}{d} \quad (\text{VIII.3})$$

Note that this equation is only valid for low concentrations. For higher concentrations, the full expression Eq.III.53 should be used. The permeation method is easy but suffers from the fact that the measured quantity is DK ; a separate determination of the solubility isotherms is thus necessary. Furthermore, permeation is a complicated phenomenon consisting of i) adsorption of H_2 at the metal surface (entry), ii) dissolution of H_2 in the form of H in the metal, iii) diffusion through the membrane, iv) recombination of two hydrogen atoms into an H_2 -molecule at the exit surface, v) finally desorption. The permeation coefficient DK is thus an average over many processes.

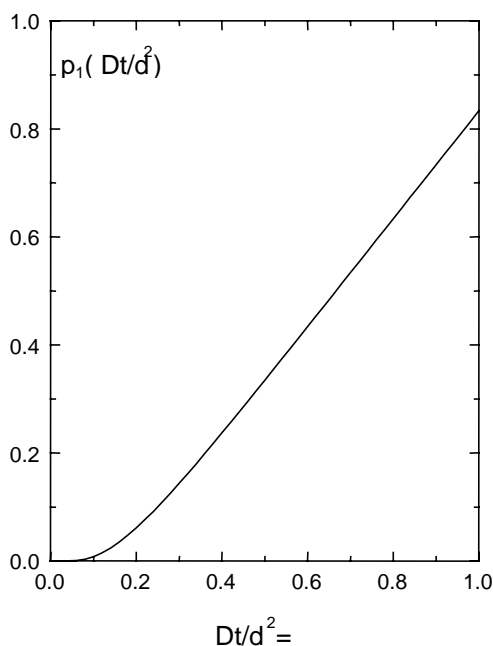


Fig. VIII.2: Time dependence of the pressure p_1 on the exit side of the membrane in a permeation experiment. Experiments of this type have been performed for example by Robertson (1973).

The permeation method is generally used in the form of the time-lag method for which at $t=0$ the pressure in the compartment on the left is suddenly increased from zero to a certain value p_2 . Then the pressure on the exit side is increasing according to (see Crank, Eq. 4.24a)

$$p_1 = \frac{kT}{V} Ad \sqrt{p_2} \left[\frac{Dt}{d^2} - \frac{1}{6} - \frac{2}{\pi^2} \sum \frac{(-1)^n}{n^2} e^{-\left(\frac{n\pi}{d}\right)^2 Dt} \right] \quad (\text{VIII.4})$$

where A is the cross-sectional area of the membrane, V the volume containing the gas at pressure p_1 and d the thickness of the membrane. In deriving Eq.VIII.4 we have assumed that the concentration remains essentially zero in the compartment on the right. For large times t ($Dt \gg d^2$), Eq.VIII.4 reduces to

$$p_1 \cong \frac{KAd}{V} \sqrt{p_2} \left[\frac{Dt}{d^2} - \frac{1}{6} \right] \quad (\text{VIII.5})$$

As can be seen in Fig.VIII.2, this is a straight line with intercept at $t=\tau$

$$\tau = \frac{d^2}{6D} \quad (\text{VIII.6})$$

D2 Electrolytic methods

Instead of gases at different pressure on both sides of the membrane, it is also possible to use electrolytes. The membrane separates then two electrolytic solutions as shown in Fig.VIII.3. By means of a potential difference between the counter electrode and the sample it is possible to load hydrogen from, say, the left side. The integrated current gives the total charge of the protons which were injected into the sample. The protons are not uniformly distributed in the sample and

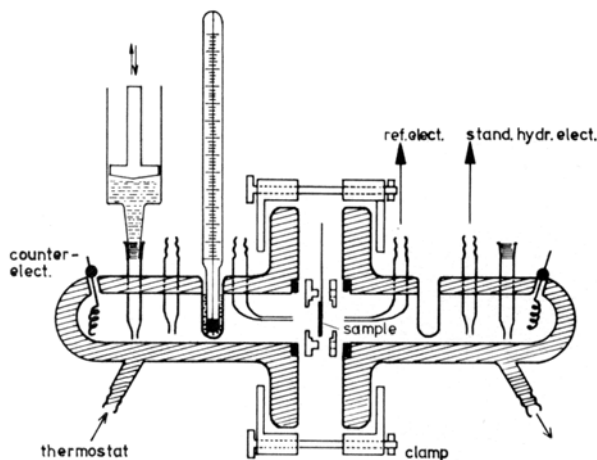


Fig. VIII.3: Electrolytic measuring cell after Boes and Züchner (1976). For clarity both sides of the cell are shown in an unclamped position. The cell is constructed symmetrically to allow for diffusion in both senses.

the concentration of H's on the left surface (entry) is higher than on the right surface (exit). The electrical potentials V_{REL-S} and V_{RER-S} (REL=reference electrode on the left) are thus different.

Without going into details let us just indicate how a potential difference V is related to the concentration of hydrogen in the sample. To do this let us assume that at $t=0$ we dip both the sample and the reference electrode RE in the electrolyte. The system being not in thermodynamical equilibrium develops a potential difference V and a current starts to flow if both the sample and RE are connected electrically outside the electrolyte. This current flows until the equilibrium is reached and $V=0$. The whole process cannot be described by means of thermodynamics. This is only possible if we connect a voltage source such that no current is flowing. If the voltage is slightly increased the current will flow from one electrode to the other say RE→sample. If the voltage is decreased the current flows from the sample to RE. In this process (which is reversible) the change in Gibbs free energy is given by

$$\delta G_H = (\mu_H - \mu_{H^+}) \delta N_H \quad (\text{VIII.7})$$

in analogy to Eq.III.6. We assume here that the H^+ ions of the electrolyte are dissolved into the metal sample. In the limit of small concentrations, we have from Eq.III.52

$$\mu_H \cong kT \ln c_H + \varepsilon_0 \quad (\text{VIII.8})$$

Thus

$$\delta G_H = \left[\varepsilon_0 - \mu_{H^+}^0 + kT \ln \left(\frac{c_H}{a_{H^+}} \right) \right] \delta N_H \quad (\text{VIII.9})$$

where we have written

$$\mu_{H^+} = \mu_{H^+}^0 + kT \ln a_{H^+} \quad (\text{VIII.10})$$

to obtain a somewhat “elegant” relation (“a” is called the activity). δG_H is the change in the Gibbs free energy when δN_H hydrogen atoms are dissolved in the metal. This is however only possible if δN_H electrons flow from the RE to the sample. The work associated with this displacement of electrons is $eV\delta N_H$. Thus

$$eV\delta N_H = \left[\varepsilon_0 - \mu_{H^+}^0 + kT \ln \frac{c_H}{a_{H^+}} \right] \delta N_H \quad (\text{VIII.11})$$

If we denote by V_R and V_L the potentials on the right and left sides of the sample and by c_{HR} and c_{HL} the corresponding surface hydrogen concentrations, then we obtain the following simple relation for the potential difference V_R-V_L is obtained

$$\Delta V = V_R - V_L = \frac{kT}{e} \ln \frac{c_{HR}}{c_{HL}} \quad (\text{VIII.12})$$

If the concentration c_{HL} is constant, then the solution of the diffusion equation is

$$c(x,t) = 1 - \frac{4}{\pi} \sum_{n=0}^{\infty} \frac{1}{2n+1} \sin\left(\frac{(2n+1)\pi x}{2L}\right) e^{-\frac{(2n+1)^2 \pi^2 Dt}{4L^2}} \quad (\text{VIII.13})$$

and the concentration c_{HR} on the right hand side of the sample increases with time according to

$$\frac{c_{HR}(t)}{c_{HL}} = 1 - \frac{4}{\pi} \sum_{n=0}^{\infty} \frac{(-1)^n}{2n+1} e^{-\frac{(2n+1)^2 \pi^2 Dt}{4L^2}} \quad (\text{VIII.14})$$

where L is the thickness of the membrane.

Both τ_b and τ_i (inflexion point) can be used to determine the diffusion constant D , since

$$\tau_b = 0.76 \frac{L^2}{\pi^2 D} \quad \text{and} \quad \tau_i = \frac{3 \ln 3}{2} \frac{L^2}{\pi^2 D} \quad (\text{VIII.15})$$

Other electrolytic methods are described by Boes and Züchner (1976).

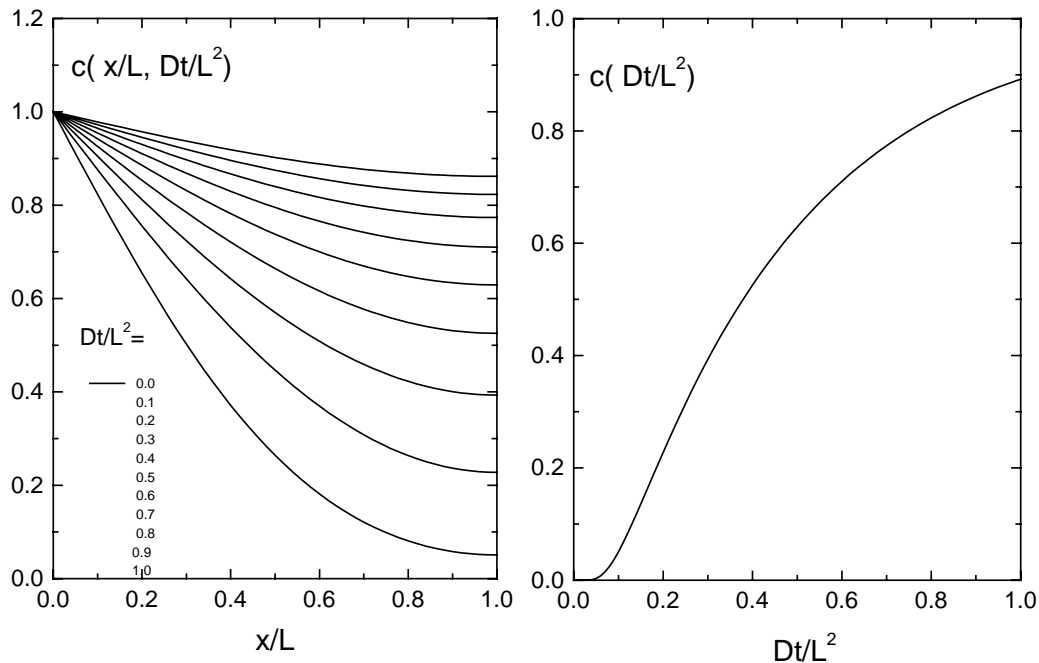


Fig. VIII.4: Time dependence of the concentration profile during hydrogen absorption in a sample of thickness L (left panel). Note that the $t=0$ curve coincides with the bottom x -axis and the left y -axis ; Time dependence of the concentration on the right face of the sample (right panel).

D3 The Gorsky effect

Although discovered by Gorsky in 1935 this effect has only been applied in the seventieth to the study of metal-hydrogen systems. A typical experimental set-up is schematically shown in Fig.IV.5. The deflection of the sample can be measured optically or capacitively. In the latter case displacements down to 1 nm can be detected

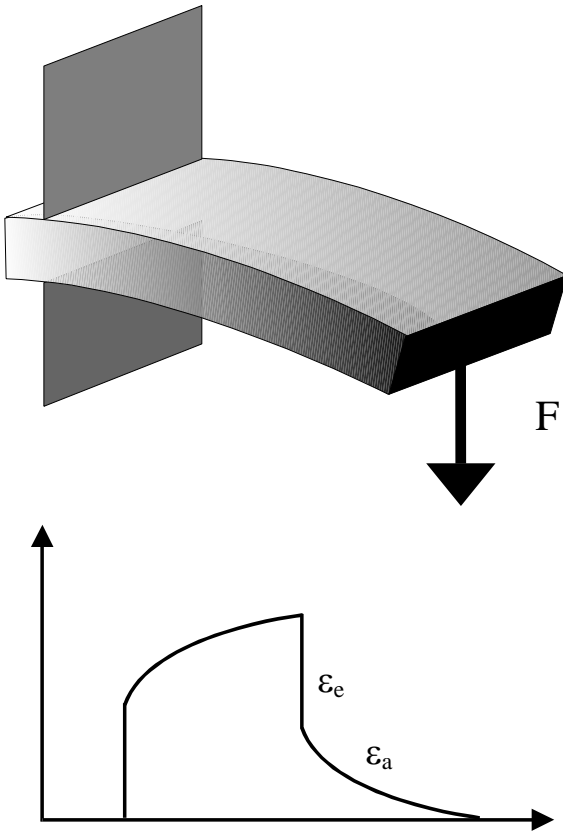


Fig. VIII.5: Schematic representation of a Gorsky experiment. The force \mathbf{F} produces a bending of the metallic beam (with a thickness d) and forces hydrogen to migrate from the compressed region to the decompressed part of the sample. In contrast to the elastic response ϵ_e which is instantaneous and proportional to \mathbf{F} , the anelastic strain ϵ_a is a slow process controlled by diffusion and the strain ϵ_a is found to reach a maximum asymptotically according to a relation of the type

$$\epsilon_a \sim e^{-t/\tau}$$

by means of a high-precision capacitance bridge (Verbruggen et al., 1984). The relation between τ and the diffusion constant D is easily obtained from

$$D = \frac{d^2}{\pi^2 \tau} \tag{ VIII.16}$$

where d is the thickness of the specimen. The result in Eq.VIII.16 follows directly from the general form of the solution of the diffusion equation

$$\frac{\partial c}{\partial t} = D \frac{\partial^2 c}{\partial x^2} \tag{ VIII.17}$$

by the method of separation of variables, which leads to functions of the form

$$\cos\left((2n+1)\pi\frac{x}{d}\right)e^{-(2n+1)^2\pi^2\frac{Dt}{d^2}} \quad (\text{VIII.18})$$

in which the dominant time dependent factor is that with $n=0$.

D4 Resistivity relaxation

In this method one makes use of the fact that the resistivity of a metal-hydrogen system increases with hydrogen content. Experimental values obtained by Simons and Flanagan (1965) for α -PdH_x are shown in Fig.IV.6. By means of local resistivity measurements one can then map out the concentration gradient. This method has been used in diffusion experiments as well as in electromigration (Erckman and Wipf, 1976) and thermomigration (Wipf and Alefeld, 1974). An example obtained in our group by Brouwer et al (1988) will be shown in the subsection on electromigration.

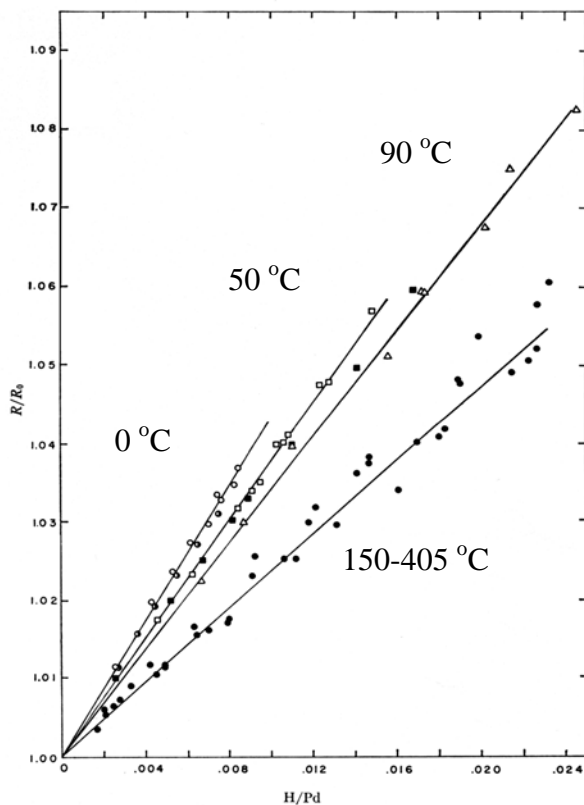


Fig. VIII.6: Relative resistivity variation R/R_0 of α -Pd-H at various temperatures. The dots • are older measurements by Lindsay and Pement (1962). All other data are from Simons and Flanagan (1966)

D5 Nuclear magnetic resonance (NMR)

It is not the purpose of this subsection to give a detailed description of nuclear magnetic resonance, but we shall just point out the basic concepts and some aspects of the use of NMR to measure diffusion constants.

NMR is basically a resonance between Zeeman-split energy levels. To illustrate this point let us consider a nucleus with angular momentum $\hbar\mathbf{I}$ and magnetic moment \mathbf{m} . We have

$$\mathbf{m} = \gamma\hbar\mathbf{I} \quad (\text{VIII.19})$$

where γ is the gyromagnetic ratio. The interaction energy of \mathbf{m} with a homogeneous magnetic field \mathcal{H} which for convenience shall be taken in the z-direction, is

$$U_{\text{int}} = -\mathbf{m} \cdot \mathbf{H} = -\gamma\hbar I_z H \quad (\text{VIII.20})$$

For a proton $I_z = \pm 1/2$ and the splitting of the spin-up and spin-down levels is

$$\Delta E = 2\left|\gamma_p \hbar \frac{1}{2} H\right| = \gamma_p \hbar H \quad (\text{VIII.21})$$

with

$$\gamma_{\text{proton}} = 2.68 \cdot 10^4 \text{ s}^{-1} \text{ G}^{-1} \quad (\text{VIII.22})$$

High frequency electromagnetic radiation of angular frequency ω_0 such that

$$\omega_0 = \gamma_p H \quad ; \omega = 2\pi\nu \quad (\text{VIII.23})$$

will be able to excite a nucleus \uparrow to a state \downarrow . According to Eq.VIII.22, for a proton

$$\nu[\text{kHz}] = 4.26H \quad [\text{G}] = 4.26H \cdot 10^{-4} [\text{Tesla}] \quad (\text{VIII.24})$$

In a semi-classical approximation we can write the equation of motion of \mathbf{m} in \mathcal{H} as follows

$$\frac{d\hbar\mathbf{I}}{dt} = \mathbf{m} \times \mathbf{H} \quad \rightarrow \quad \frac{d\mathbf{m}}{dt} = \gamma\mathbf{m} \times \mathbf{H} \quad (\text{VIII.25})$$

On a macroscopic scale we are interested in the magnetisation $\mathbf{M} = \sum_i \mathbf{m}_i / V$ (where the summation is taken over all nuclei in the volume V). If we neglect the interactions between nuclear moments we obtain immediately the following equation of motion for \mathbf{M}

$$\frac{d\mathbf{M}}{dt} = \gamma\mathbf{M} \times \mathbf{H} \quad (\text{VIII.26})$$

At equilibrium \mathbf{M}_{eq} is parallel to \mathcal{H} and in the limit of small fields and high temperatures (more exactly when $|\mathbf{m}|\mathcal{H}/k_B T \ll 1$) we have

$$\mathbf{M}_{eq} = \chi \mathbf{H} \quad (\text{VIII.27})$$

where χ is the susceptibility.

If the system is not in thermodynamical equilibrium we have to modify Eq.VIII.25 in order to insure that for $t \rightarrow \infty$ $\mathbf{M} \rightarrow \mathbf{M}_{eq}$. As a result of the cylindrical symmetry of the problem we have to make a distinction between the cases where i) $\mathbf{M} \rightarrow \mathbf{M}_{eq}$ is parallel to \mathcal{H} and ii) $\mathbf{M} \rightarrow \mathbf{M}_{eq}$ is perpendicular to \mathcal{H} . The simplest generalisation of Eq.VIII.25 is then the set of Bloch equations

$$\frac{dM_z}{dt} = \gamma (\mathbf{M} \times \mathbf{H})_z + \frac{(M_{eq} - M_z)}{T_1} \quad (\text{VIII.28})$$

$$\frac{dM_i}{dt} = \gamma [\mathbf{M} \times \mathbf{H}]_i - \frac{M_i}{T_2} \quad i = x, y \quad (\text{VIII.29})$$

where T_1 is the spin-lattice relaxation time and T_2 is the transverse relaxation time. The Bloch equations imply that M_z relaxes as e^{-t/T_1} towards M_{eq} and M_x (and M_y) as e^{-t/T_2} towards zero. Let us now solve the Bloch equations for the important case where the magnetic field is

$$\mathbf{H} = (h \cos \omega t, -h \sin \omega t, H_0) \quad (\text{VIII.30})$$

which corresponds to the situation where a circularly polarised field h is superimposed to a large static and homogeneous field \mathcal{H}_0 . Introducing Eq.VIII.30 in Eqs.VIII.28 and 29, we obtain

$$\begin{aligned} \frac{dM_x}{dt} &= \gamma H_0 M_y + \gamma h M_z \sin \omega t - \frac{M_x}{T_2} \\ \frac{dM_y}{dt} &= \gamma H_0 M_x + \gamma h M_z \cos \omega t - \frac{M_y}{T_2} \\ \frac{dM_z}{dt} &= \gamma h (M_x \sin \omega t + M_y \cos \omega t) + \frac{M_{eq} - M_z}{T_1} \end{aligned} \quad (\text{VIII.31})$$

For $h \ll \mathcal{H}_0$ one expects that \mathbf{M} will precess around \mathcal{H}_0 and $\langle M_x \rangle = \langle M_y \rangle \ll M_z$. In a steady state $dM_z/dt = 0$ (however, $dM_x/dt \neq 0$, $dM_y/dt \neq 0$) and thus $M_z = M_{eq}$. From Eq.VIII.31 we have also

$$\begin{aligned} \frac{d^2 M_x}{dt^2} &= \gamma H_0 \left[-\gamma H_0 M_x + \gamma h M_{eq} \cos \omega t - M_y / T_2 \right] \\ &+ \gamma h M_{eq} \omega \cos \omega t - \frac{1}{T_2} \frac{dM_x}{dt} \end{aligned} \quad (\text{VIII.32})$$

$$\begin{aligned} & \frac{d^2 M_x}{dt^2} + \frac{2}{T_2} \frac{dM_x}{dt} + \left(\omega_0^2 + \frac{1}{T_2^2} \right) M_x \\ & = M_{eq} \omega_1 \left[(\omega_0 + \omega) \cos \omega t + \frac{1}{T_2} \sin \omega t \right] \end{aligned} \quad (\text{VIII.33})$$

with $\omega_0 = \gamma \mathcal{H}_0$ and $\omega_1 = \gamma h$.

Without solving this equation one can write in analogy with the problem of mechanical resonance that the resonance width is $1/T_2$. Thus

$$\Delta\omega = \frac{1}{T_2} \quad (\text{VIII.34})$$

This equation can also be interpreted as an uncertainty relation where $\hbar\Delta\omega$ is the uncertainty in the energy of a level. What is the origin of this uncertainty? In many cases $\Delta\omega$ is caused by the dipole-dipole interaction of the nuclear spins with each other.

The magnetic field at the position of a given nucleus “i” is the sum of the dipolar fields of all the other nuclei and the external field \mathcal{H} . Thus

$$\mathbf{H}_i = \mathbf{H}_0 + \sum_{j \neq i} \frac{3\mathbf{r}_{ij}(\boldsymbol{\mu}_j \cdot \mathbf{r}_{ij}) - \boldsymbol{\mu}_j |\mathbf{r}_{ij}|^2}{|\mathbf{r}_{ij}|^5} \equiv \mathbf{H}_0 + \Delta\mathbf{H}_i \quad (\text{VIII.35})$$

We shall now show that the diffusion constant of, say a proton (hydrogen) or deuteron (deuterium) can be determined by measuring $\Delta\omega$ as function of temperature. For simplicity let us consider a linear system with all the \mathcal{H}_i parallel to each other but with $\mathcal{H}_i = \mathcal{H}_0 \pm \Delta\mathcal{H}_0$ (see Fig.IV.7).

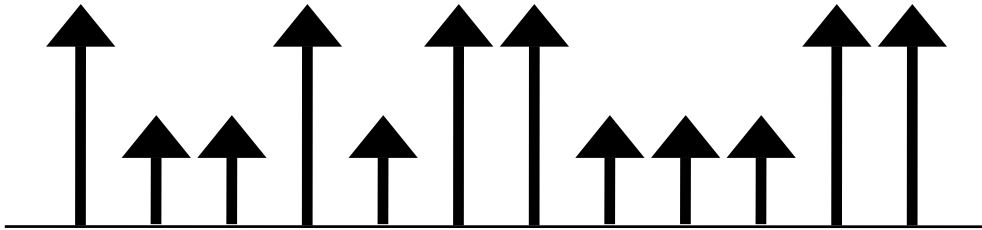


Fig. VIII.7: Linear model for a random distribution of nuclear fields. There are as many $\mathcal{H}_0 + \Delta\mathcal{H}_0$ as $\mathcal{H}_0 - \Delta\mathcal{H}_0$

The width of the resonance is

$$\Delta\omega_0 = \gamma_p \sqrt{\frac{1}{N} \sum_{j=1}^N (\mathbf{H}_j - \mathbf{H}_0)^2} = \gamma_p \Delta\mathbf{H}_0 \quad (\text{VIII.36})$$

What does one expect if the proton under investigation is not frozen-in in the lattice but hops from one interstitial to the other every τ seconds, T_2 being the lifetime of a nuclear moment, the proton will jump $n=T_2/\tau$ times during its life (in fact T_2 is the lifetime of the magnetisation, but we shall assume that it also applies to the individual nucleus). The average field $\langle \mathcal{H} \rangle$ seen by the proton is then

$$\langle \mathbf{H} \rangle = \frac{1}{n} \sum_{s=1}^n \mathbf{H}_s \quad (\text{VIII.37})$$

and

$$\Delta\mathbf{H} \equiv \sqrt{\langle (\langle \mathbf{H} \rangle - \mathbf{H}_0)^2 \rangle} = \sqrt{\left\langle \left(\frac{\sum_{s=1}^n \mathbf{H}_s - \mathbf{H}_0}{n} \right)^2 \right\rangle} = \sqrt{\left\langle \left(\frac{n_+ - n_-}{n} \Delta\mathbf{H}_0 \right)^2 \right\rangle} \quad (\text{VIII.38})$$

where n_+ is the number of sites with $\mathcal{H}_0 + \Delta\mathcal{H}_0$ seen by the hopping proton during his n -jump travel. Thus

$$n = n_+ + n_- \quad (\text{VIII.39})$$

Setting $n_+ - n_-/n = x$, $-1 \leq x \leq 1$ we can write the number of possible travels with a given number of n_+ jumps as follows

$$\eta(n, n_+) = \frac{n!}{n_+! n_-!} \cong \frac{n^n}{n_+^{n_+} n_-^{n_-}} = \frac{n^n}{\left[\frac{n}{2}(1+x) \right]^{\frac{n}{2}(1+x)} \left[\frac{n}{2}(1-x) \right]^{\frac{n}{2}(1-x)}} = \eta(n, x) \quad (\text{VIII.40})$$

$$\begin{aligned} \ln \eta(n, x) &= \frac{n}{2} [\ln 4 - (1+x) \ln(1+x) - (1-x) \ln(1-x)] \\ &\cong \frac{n}{2} [\ln 4 - x^2] \end{aligned} \quad (\text{VIII.41})$$

$$\langle x^2 \rangle = \frac{1}{n} \quad (\text{VIII.42})$$

Thus

$$\eta(n, x) \sim e^{-\frac{nx^2}{2}} \quad (\text{VIII.43})$$

and

$$\Delta\omega = [\Delta\omega_0]^2 \tau \quad (\text{VIII.44})$$

where $\Delta\omega_0 = \gamma\Delta\mathcal{H}$ is the linewidth for a system of nuclei jumping $1/\tau$ times per second from an interstitial place to another. Equation VIII.44 implies that the linewidth decreases when the jump frequency increases. In other words $\Delta\omega$ decreases with increasing temperature. This is however only valid when $x \ll 1$ or equivalently when $\tau \ll T_2$ (at 0 K). The behaviour of the linewidth predicted by Eq.VIII.44 is in good agreement with experimental data obtained in many different systems. As an example we indicate the results of early experiments by Stalinsky et al. 1961 in Fig. VIII.8.

Despite the simplicity of the model used in deriving Eq.VIII.44 it turns out that more sophisticated theoretical calculations such as that of Kubo and Tomita (1954) which predict that

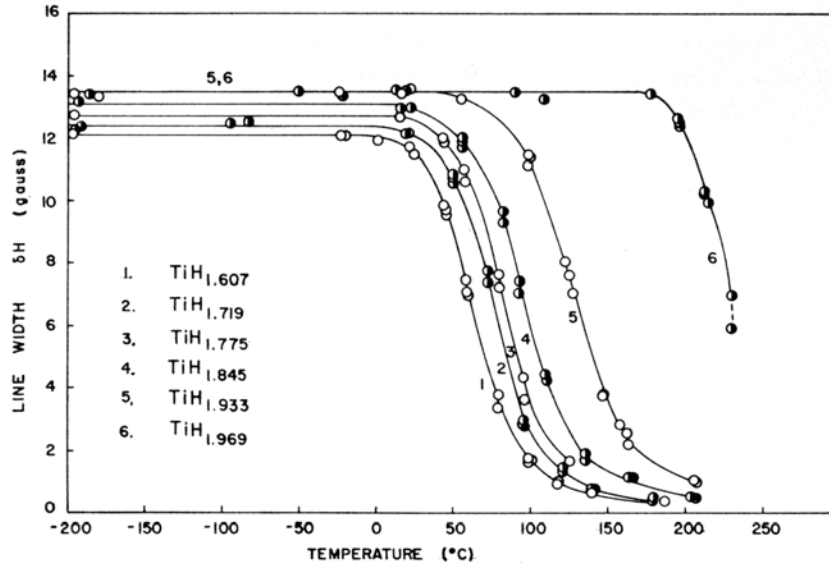


Fig. VIII.8: Motional narrowing for the proton NMR line in TiH_x (Stalinsky et al 1961).

$$\frac{1}{\tau} = \frac{\pi/2 \Delta\omega}{4 \ln 2 \tan\left(\frac{\pi}{2} \left(\frac{\Delta\omega}{\Delta\omega_0}\right)^2\right)} \quad (\text{VIII.45})$$

give essentially the same result in the limit $\Delta\omega < \Delta\omega_0$ as can be seen by linearizing Eq.VIII.45

$$\frac{1}{\tau} = \frac{1}{4 \ln 2} \frac{(\Delta\omega_0)^2}{\Delta\omega} \cong 0.4 \frac{(\Delta\omega_0)^2}{\Delta\omega} \quad (\text{VIII.46})$$

We are not going to consider NMR-techniques in more detail as the main purpose of this subsection was just to demonstrate the relation which exists between nucleus motion and NMR line-width. The interested reader is referred to the review paper by Cotts (1978).

D6 Quasi-elastic neutron diffraction

A neutron interacts mainly with the nuclei (and not with the electrons) when it's separation from a given nucleus is $\sim 10^{-14}$ m. For studies of solids one uses neutrons with energies of the order of 0.05 eV with a wavelength of $\sim 2\text{\AA}$. For most purposes one can thus assume that the neutron described by the incoming plane wave

$$\Psi_{in}(\mathbf{r}) = \left(\frac{\hbar|\mathbf{k}_0|}{m_n}\right)^{-1/2} e^{-i\mathbf{k}_0 \cdot \mathbf{r}} \quad (\text{VIII.47})$$

is scattered by a point-like potential, such that

$$\Psi_{out}(\mathbf{r}) = -b \left(\frac{\hbar|\mathbf{k}_0|}{m_n}\right)^{-1/2} \frac{e^{i\mathbf{k} \cdot \mathbf{r}}}{r} \quad (\text{VIII.48})$$

where $\hbar\mathbf{k}_0 = m_n \mathbf{v}_0$ and b is the scattering length which is in general a complex number, \mathbf{v}_0 is the velocity of the incoming neutrons and $\hbar\mathbf{k}$ is the momentum of the outgoing neutrons. In an elastic scattering $\mathbf{k} = \mathbf{k}_0$; in quasi-elastic scattering $\mathbf{k} \approx \mathbf{k}_0$, i.e. the energy is only slightly modified by the scattering process.

If we have many scattering centres (e.g. the protons in a metal-hydride alloy) then the total outgoing function is

$$\Psi_{out}(\mathbf{r}) = -\left(\frac{\hbar|\mathbf{k}_0|}{m_n}\right)^{-1/2} \frac{e^{i\mathbf{k} \cdot \mathbf{r}}}{r} \sum_{l=1}^N P_l b_l e^{i\mathbf{k} \cdot \mathbf{r}_l} \quad (\text{VIII.49})$$

where N is the number of interstitial sites in the crystal and P_l indicates the probability of having a particular site \mathbf{r}_l occupied by a proton

$$\boldsymbol{\kappa} = \mathbf{k} - \mathbf{k}_0 \quad (\text{VIII.50})$$

Let us first consider the case where $P_1=1$ for every interstitial site. Even in this case it is found that the b_l are not identical because of the different nuclear spins of the scatterer. This has an important consequence for the differential effective cross section $d\sigma/d\Omega$ (number of neutrons scattered in directions around \mathbf{k} in space angle $d\Omega$ per second per scatterer)

$$\frac{d\sigma}{d\Omega} = |\Psi_{out}(\boldsymbol{\kappa})|^2 r v_0 = \frac{1}{N} \left| \sum_{l=1}^N b_l e^{i\boldsymbol{\kappa} \cdot \mathbf{r}_l} \right|^2 = \underbrace{\overline{|b|^2} - |\bar{b}|^2}_{incoherent} + \underbrace{|\bar{b}|^2}_{coherent} \frac{1}{N} \sum_{l=1}^N e^{i\boldsymbol{\kappa} \cdot \mathbf{r}_l} \quad (\text{VIII.51})$$

The so-called *coherent* part is responsible for interference phenomena (Bragg reflections) while the *incoherent* does not show any characteristic behaviour.

For inelastic scattering one finds a relation which is very similar to Eq.IV.47 for the double effective cross-section

$$\frac{d^2\sigma}{d\Omega d\omega} = \frac{k}{k_0} \left\{ |\bar{b}|^2 S(\boldsymbol{\kappa}, \omega) + \left(\overline{|b|^2} - |\bar{b}|^2 \right) S_s(\boldsymbol{\kappa}, \omega) \right\} \quad (\text{VIII.52})$$

where $\hbar\omega$ is the energy of a neutron.

We have assumed, so far, that $P_1=1$ for all sites. If however $P_1 \neq 1$ for certain sites then one expects that the functions $S(\boldsymbol{\kappa}, \omega)$ and $S_s(\boldsymbol{\kappa}, \omega)$ will depend both on the space and time variation of $P_1=P_1(\mathbf{r}_1, t)$. From the fact that $\boldsymbol{\kappa}$ and ω are the Fourier conjugate of \mathbf{r}_1 and t it is not surprising that

$$S_s(\boldsymbol{\kappa}, \omega) \sim \iint d^3r dt e^{i(\boldsymbol{\kappa} \cdot \mathbf{r} - \omega t)} P(\mathbf{r}, t) \quad (\text{VIII.53})$$

We assume now that the probability $P(\mathbf{r}, t)$ of finding a proton at position \mathbf{r} and time t is related to the probabilities $P(\mathbf{r} + \mathbf{s}_j, t)$ of finding a proton on nearest neighbour interstitial sites by the following expression

$$\frac{\partial P(\mathbf{r}, t)}{\partial t} = \frac{\frac{1}{n_0} \sum_{j=1}^{n_0} P(\mathbf{r} + \mathbf{s}_j, t) - P(\mathbf{r}, t)}{\tau} \quad (\text{VIII.54})$$

We shall show later that Eq.VIII.54 is in fact just the diffusion equation written in terms of occupation probability. n_0 is the number of nearest neighbours. The time τ is to be considered as an empirical parameter (relaxation time). We shall show later that it is closely related to the diffusion constant. Let us now Fourier transform Eq.VIII.54 in two steps. we have, first

$$\frac{\partial \int d^3r P(\mathbf{r}, t) e^{i\boldsymbol{\kappa} \cdot \mathbf{r}}}{\partial t} = \frac{\frac{1}{n_0} \sum_{j=1}^{n_0} \int d^3r P(\mathbf{r} + \mathbf{s}_j, t) e^{i\boldsymbol{\kappa} \cdot \mathbf{r}} - \int d^3r P(\mathbf{r}, t) e^{i\boldsymbol{\kappa} \cdot \mathbf{r}}}{\tau} \quad (\text{VIII.55})$$

Defining the function $I(\boldsymbol{\kappa}, t)$ by means of

$$I(\mathbf{\kappa}, t) = \int d^3r P(\mathbf{r}, t) e^{i\mathbf{\kappa} \cdot \mathbf{r}} \quad (\text{VIII.56})$$

we see that Eq.VIII.55 can be written in terms of $I(\mathbf{\kappa}, t)$ as follows

$$\frac{\partial I(\mathbf{\kappa}, t)}{\partial t} = \left(\frac{1}{n_0} \sum_{j=1}^{n_0} e^{-\mathbf{\kappa} \cdot \mathbf{s}_j} - 1 \right) \frac{I(\mathbf{\kappa}, t)}{\tau} \quad (\text{VIII.57})$$

which implies that

$$I(\mathbf{\kappa}, t) = e^{-t/\tau \left(\frac{1}{n_0} \sum_{j=1}^{n_0} e^{-i\mathbf{\kappa} \cdot \mathbf{s}_j} - 1 \right)} \quad (\text{VIII.58})$$

We have then

$$\begin{aligned} S_s(\mathbf{\kappa}, \omega) &\sim \int dt I(\mathbf{\kappa}, t) e^{-i\omega t} \\ &= 2 \frac{f(\mathbf{\kappa}) / \tau}{\omega^2 + (|f(\mathbf{\kappa})| / \tau)^2} \end{aligned} \quad (\text{VIII.59})$$

since

$$\int_{-\infty}^{\infty} dt e^{-i\omega t} e^{-\gamma t} = 2 \frac{\gamma}{\omega^2 + |\gamma|^2} \quad (\text{VIII.60})$$

This is a Lorentzian curve with a width at half height $\Delta\omega = 2f(\mathbf{x}) / \tau$. In the limit $|\mathbf{x}| \rightarrow 0$

$$\lim_{|\mathbf{\kappa}| \rightarrow 0} f(\mathbf{\kappa}) = -\frac{|\mathbf{\kappa}|^2 S^2}{6} \quad (\text{VIII.61})$$

in the simple case where the interstitial sites form a simple-cubic structure. We have then

$$\Delta\omega = 2|\mathbf{\kappa}|^2 \frac{S^2}{6\tau} = 2D|\mathbf{\kappa}|^2 \quad (\text{VIII.62})$$

where the diffusion constant D is set equal to

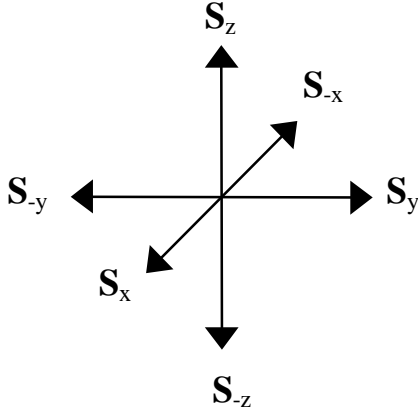
$$D = \frac{S^2}{6\tau} \quad (\text{VIII.63})$$

Relation Eq.VIII.63 can be derived as follows. The diffusion equation

$$\frac{\partial c}{\partial t} = D\Delta c \quad \text{with} \quad \Delta = \frac{\partial^2}{\partial x^2} + \frac{\partial^2}{\partial y^2} + \frac{\partial^2}{\partial z^2} \quad (\text{VIII.64})$$

is also valid for the probability function $P(\mathbf{r}, t)$

$$\frac{\partial P}{\partial t} = D \left(\frac{\partial^2 P}{\partial x^2} + \frac{\partial^2 P}{\partial y^2} + \frac{\partial^2 P}{\partial z^2} \right) \quad (\text{VIII.65})$$



$$\begin{aligned} \frac{\partial^2 P}{\partial x^2} &= \frac{1}{s} \left\{ \frac{[P(\mathbf{r} + \mathbf{s}_x) - P(\mathbf{r})]}{s} - \frac{[P(\mathbf{r}) - P(\mathbf{r} + \mathbf{s}_{-x})]}{s} \right\} \\ &= \frac{1}{s^2} \{ P(\mathbf{r} + \mathbf{s}_x) + P(\mathbf{r} + \mathbf{s}_{-x}) - 2P(\mathbf{r}) \} \end{aligned} \quad (\text{VIII.66})$$

Similar relations are obtained for the y and z directions. Thus

$$\begin{aligned} \frac{\partial P}{\partial t} &= \frac{D}{s^2} \left\{ \sum_j P(\mathbf{r} + \mathbf{s}_j) - 6P(\mathbf{r}) \right\} \\ &= \frac{6D}{s^2} \left\{ \frac{1}{6} \sum_j P(\mathbf{r} + \mathbf{s}_j) - P(\mathbf{r}) \right\} \end{aligned} \quad (\text{VIII.67})$$

Equation VIII.63 follows then from Eqs.VIII.54 and 67. From Eq.VIII.62 it follows that the width in energy of a quasi-elastic neutron diffraction peak is a measure of the diffusion constant D . This result can also be viewed as a consequence of Heisenberg's uncertainty relations for energy and momentum. The argument goes as follows. Let us assume that the mean residence time of a proton on a given interstitial site is τ . The scattering of an incoming neutron has then to take place in τ seconds. This leads to a energy uncertainty $\hbar\Delta\omega \cong 1/\tau$. Furthermore we know that

the proton is localised in a box of dimension $s \times s \times s$. This implies that the momentum of the proton, κ is such that

$$\kappa_x \cdot s \cong 1 \quad \kappa_y \cdot s \cong 1 \quad \kappa_z \cdot s \cong 1 \quad (\text{VIII.68})$$

From Eq.IV.59 and Eq.IV.63 and the fact that $x_x^2 = x_y^2 = x_z^2 = \frac{1}{3}|\kappa|^2$ we obtain then

$$\hbar\Delta\omega = 2\hbar D|\kappa|^2 \quad (\text{VIII.69})$$

in perfect agreement with Eq.VIII.62. The parabolic behaviour of $\hbar\Delta\omega$ at low momentum transfer is nicely shown in Figs.IV.9 and IV.10 in which the quasielastic line width is plotted as a function of the momentum transfer κ . The fitted curves are obtained by evaluating $f(\mathbf{x})$ for tetrahedral-tetrahedral diffusion jumps,

$$f(\kappa \parallel [100]) = \frac{1}{3} \left(1 - \cos \frac{a\kappa}{2} \right)$$

$$f(\kappa \parallel [110]) = \frac{2}{3} \left(1 - \cos \frac{a\kappa}{2\sqrt{2}} \right) \quad (\text{VIII.70})$$

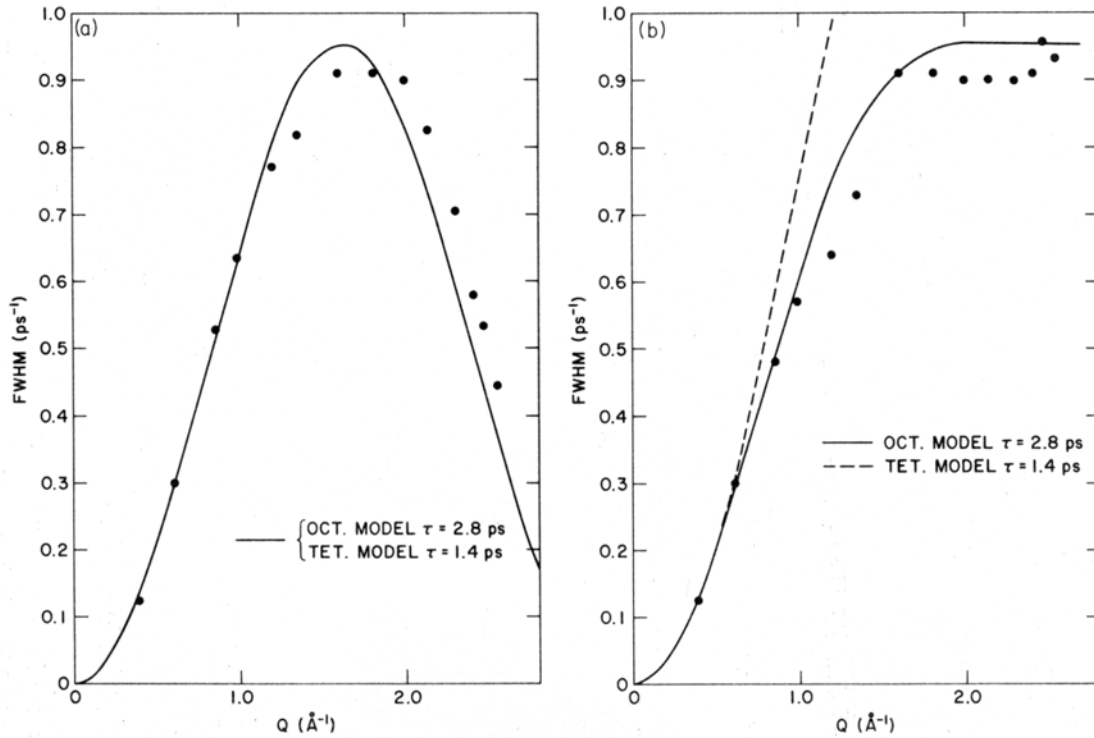


Fig. VIII.9: Linewidth for neutrons scattered quasi-elastically on hydrogen in $\text{PdH}_{0.03}$ at $T=623$ K as measured by Rowe et al (1972). The left panel is for κ parallel to $[100]$ and the right panel for κ parallel to $[110]$. The time τ is indicated in picoseconds.

and for octahedral-octahedral diffusion jumps

$$f(\kappa \parallel [100]) = \frac{2}{3} \left(1 - \cos \frac{a\kappa}{2} \right)$$

$$f(\kappa \parallel [100]) = \frac{1}{3} \left(3 - \cos^2 \frac{a\kappa}{2\sqrt{2}} - 2 \cos \frac{a\kappa}{2\sqrt{2}} \right)$$
(VIII.71)

The fit is much better for octahedral-octahedral jumps than tetrahedral-tetrahedral jumps. This implies that in dilute Pd-H (α) diffusion goes via octahedral-octahedral jumps.

D7 Optical methods

In a recent article we demonstrated (den Broeder et al. (1998) that diffusion of hydrogen could be monitored visually in samples with a special configuration that allows hydrogen absorption locally. The samples needed for this type of experiments are produced in the following way. First a typically 300 nm thick yttrium film is evaporated under UHV conditions on top of a transparent substrate (sapphire or silica) by means of an electron gun. Subsequently, a 30 nm thick palladium pattern (e.g. a disk or a set of strips) is evaporated in-situ on top of the Y. In air, the yttrium oxidises forming a 100 nm Y_2O_3 -layer (as determined by Rutherford backscattering), which is impermeable to hydrogen atoms. However, areas covered with Pd do not oxidise, opening the possibility for hydrogen to permeate through the Y/Pd boundary (see top panel of Fig. VIII.10).

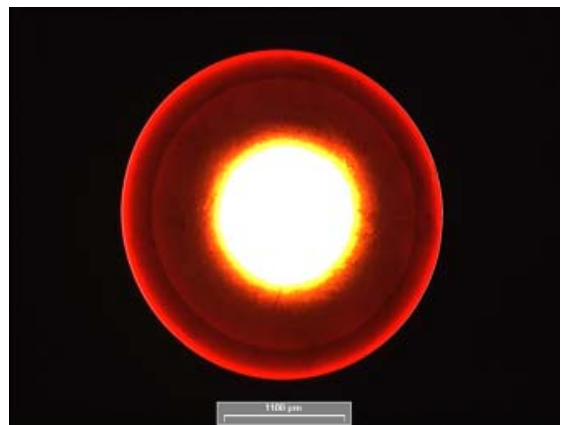
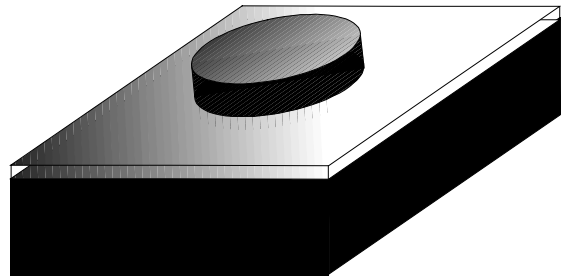


Fig. VIII.10: The diffusion of hydrogen in YH_x can be observed visually since the optical properties of this hydride depend strongly on its concentration. For the circular geometry considered in this experiment the bright red outer circle corresponds to the α - β phase boundary between dilute YH_x and the dihydride $YH_{2-\delta}$ while the white central disk corresponds to the trihydride $YH_{3-\delta}$. The diameter of the Pd disk is 1 mm. At 400 K hydrogen diffuses approximately 100 μm per second.

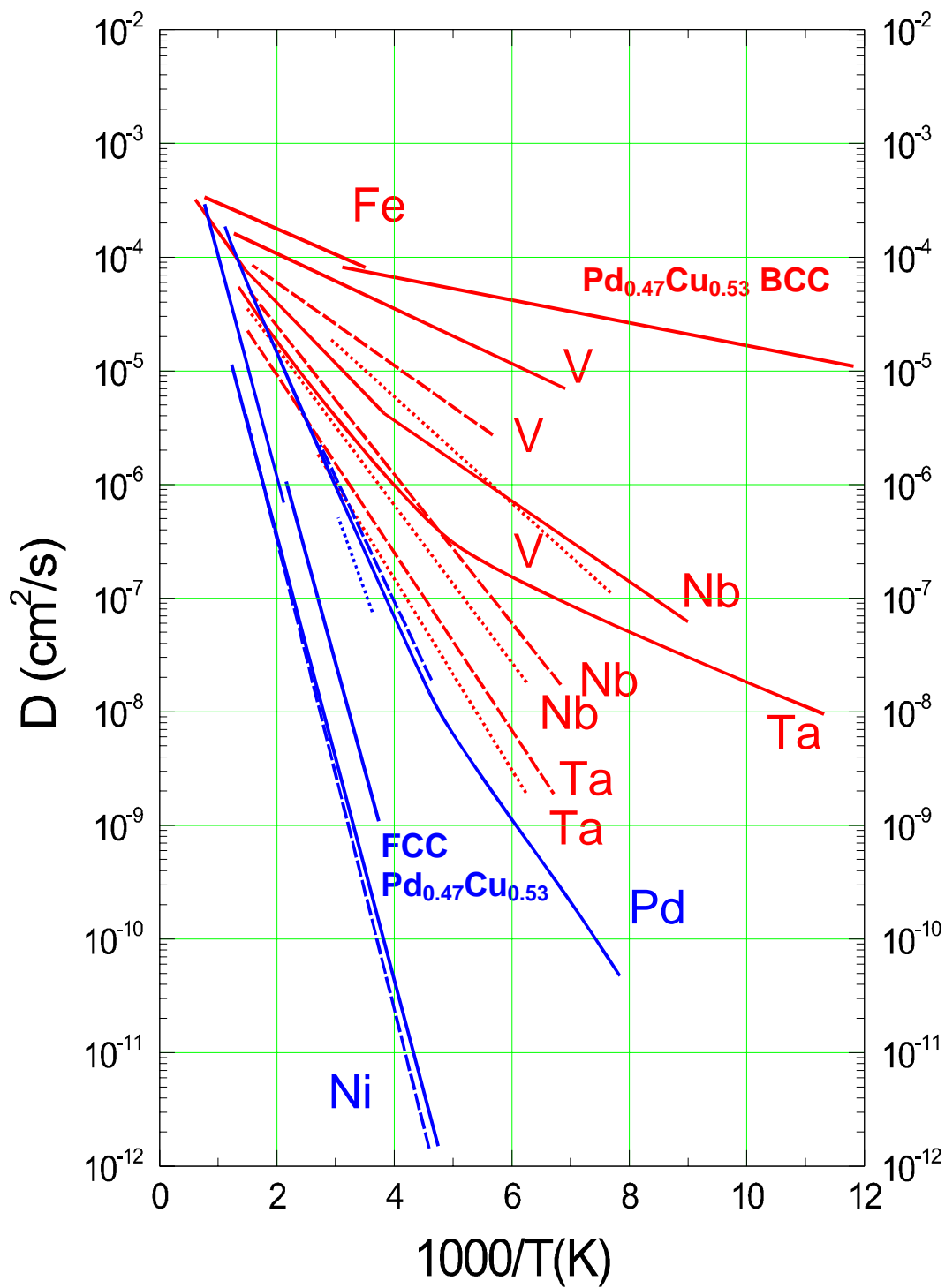


Fig. VIII.11: Temperature dependence of the diffusion coefficient for hydrogen (full line), deuterium (dashed line) and tritium (dotted line) in FCC metals (blue curves) and in BCC metals (red curves). The host metals are indicated by their symbols. Note the extreme influence of the crystal structure in the case of the PdCu alloy.

In a typical experiment H_2 gas (at 10^5 Pa) is introduced into the chamber containing the sample. The chamber is equipped with optical windows and a temperature control system and can be placed onto the positioning table of an optical microscope. Using a white lamp at the back side of the cell, optical transmission changes are monitored by means of a CCD colour camera. In contact with hydrogen gas, the yttrium underneath the palladium pattern immediately starts absorbing hydrogen atoms, because Pd is an excellent catalyst for H_2 dissociation. Therefore, within a few seconds a transparent $YH_{3-\delta}$ area is formed in the Pd covered region (see Fig. 1a). Further hydrogen uptake can only take place if H diffuses out laterally, i.e. into the Y underneath the transparent Y_2O_3 -layer (see lower panel of Fig.IV.10).

As a function of time radial hydrogen diffusion leads to a concentration gradient which can directly be observed optically. This offers a wealth of interesting possibilities.

A wealth of data on the diffusion of hydrogen in metals has been accumulated during the last decades. In Figs.IV.11 and 12 we indicate data for FCC and BCC metals. It is immediately apparent that the diffusion of hydrogen in BCC metals is in general faster than in FCC metals. Especially fast is the diffusion in vanadium and in iron. However, one should realise that Fe in contrast to V absorbs only very small amounts of hydrogen. Another interesting phenomenon is the reverse isotope effect observed in Pd. In this metal the heavy deuterium (D) diffuses faster than the light hydrogen !

ELECTROMIGRATION: EXPERIMENTAL METHODS

In almost all methods used to determine the electromigration of hydrogen in a metal one measures the effect of an electrical current on an initially homogeneous concentration distribution of hydrogen atoms. The most widely used methods are:

- Flow methods (E1)
- Internal flow method (E2)
- Concentration gradient method (E3)
- Dilatometric method (E4)
- Optical method (E5)

Before describing briefly these methods we indicate in Fig.IV.13 how the hydrogen concentration is influenced as a function of time t by an electrical current flowing through a sample of length L . The concentration c is constant throughout the sample before the current is turned on. As soon as a current is passed through the sample a depletion zone develops on the left while an accretion zone is formed on the right. The migration of hydrogen proceeds until a stationary state is reached. In the stationary state the electrical force is exactly balanced by the concentration gradient which drives the particle to the left. The problem is mathematically identical to that of the (isothermal) atmosphere in the gravitational field of the Earth.

As we shall show in the theory of irreversible processes the particle (hydrogen) current J is directly proportional to the force acting on the particles of effective charge Z^* and to the gradient of the chemical potential μ_H i.e.

$$\mathbf{J} = L_{HH} (eZ^* \mathbf{E} - \text{grad} \mu_H) \quad (\text{VIII.72})$$

where \mathbf{E} is the electrical field induced by the electron current and the parameter L_{HH} is related to the diffusion coefficient through

$$L_{HH} = D \left(\frac{\partial \mu_H}{\partial \rho_H} \right)^{-1} \cong D \left(\frac{kT}{\rho_H} \right)^{-1} \quad (\text{VIII.73})$$

In combination with the continuity equation for hydrogen atoms

$$\frac{\partial c}{\partial t} + \text{div} \mathbf{J} = 0 \quad (\text{VIII.74})$$

Eqs. VIII.72 and 73 lead to

$$\frac{\partial c}{\partial t} = D \frac{\partial^2 c}{\partial x^2} - MeZ^* \mathbf{E} \frac{\partial c}{\partial x} \quad (\text{VIII.75})$$

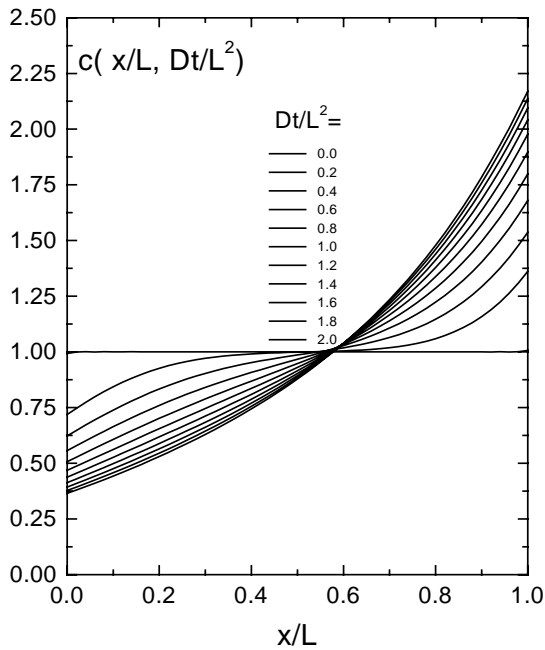


Fig.VIII.12: Time dependence of the hydrogen concentration profile in a sample of length L through which a constant electrical current is passed (electromigration).

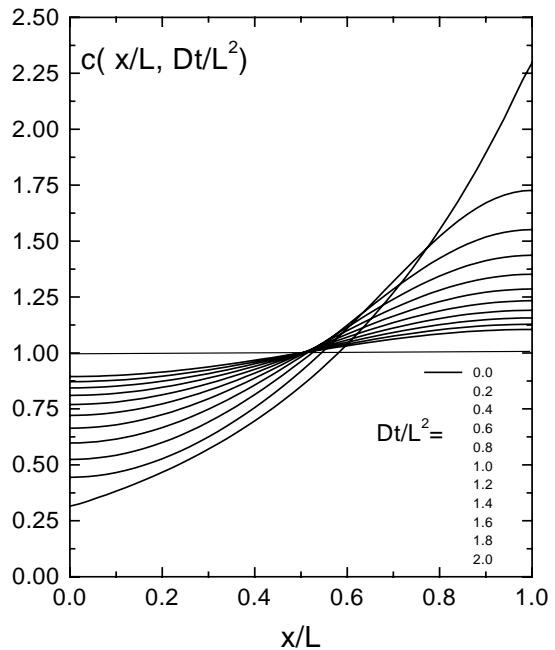


Fig.VIII.13: Time dependence of the hydrogen concentration profile in the sample of Fig.VIII.12 after the electrical current has been reduced to zero (relaxation).

where the mobility M is related to the diffusion coefficient by the generalized Einstein relation by

$$D = Mc \frac{\partial \mu}{\partial c} \quad (\text{VIII.76})$$

At low concentration $D = MkT$

$$\frac{\partial c}{\partial t} = D \frac{\partial^2 c}{\partial x^2} - MeZ^* \mathbf{E} \frac{\partial c}{\partial x} \quad (\text{VIII.77})$$

This equation is very useful to investigate the effect of an electric field on the hydrogen distribution in a sample at low hydrogen concentration. It is, however, not adequate for the description of hydrogen migration in switchable mirrors since in these MH_x systems the hydrogen concentration varies often from $x=0$ to $x=3$. Equation VIII.76 has been used for the calculations shown in Fig.VIII.12. The stationary state is a simple exponential function. From Eq.VIII.77 one can also calculate the relaxation of the stationary state when the current is suddenly reduced to zero, i.e. when $\mathbf{E}=0$. One obtains then the concentration profiles in Fig.VIII.13. Interesting is that during relaxation there is a region (around $x/L=0.6$) in the sample in which the hydrogen concentration increases first before decreasing to zero.

E1 Flow measurements

The principle of this method is shown in Fig.VIII.14. A strong current is passed through the sample and produces the migration of hydrogen from one side of the sample to the other. This transport of hydrogen increases the pressure of H_2 -gas on the right and displaces the oil drop, the velocity of which is proportional to the hydrogen flow. for small concentrations. In the situation shown in Fig.IV.15, $\text{grad}\mu_H=0$ because H is assumed to enter freely the sample. Thus

$$|\mathbf{J}| = \frac{e|Z^*| \rho_0 IA(DK) \sqrt{p}}{kT} \quad (\text{VIII.78})$$

where $(D \cdot K)$ is the permeability of H in the sample under consideration (see Eq.IV.3), ρ_0 is the electrical specific resistivity, Z^* is the effective charge number of H in the sample, k is the Boltzmann constant and $p^{1/2}$ comes from the use of Sievert's law (see Eq.II.34 and Eq.IV.2). A is the cross-sectional area of the sample. The expression Eq.VIII.78 shows that the effective charge number Z^* of a migrating ion may be determined by measuring the ion flow J and the permeability. Details of the apparatus used by Einziger and Huntington (1974) (which was very similar to that of Oriani and Gonzalez (1967) (H in Pd)) is shown in Fig.VIII.14.

A similar apparatus has been used by Marêché et al (1977) to study electromigration in $Nb-H$, $V-$

H and Ta-H.

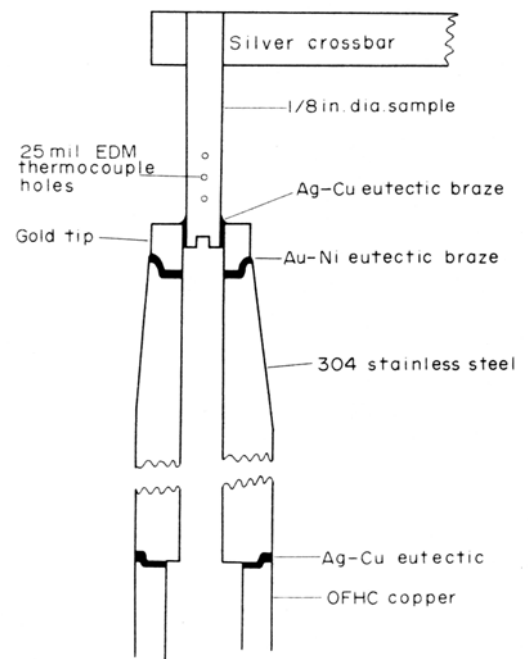
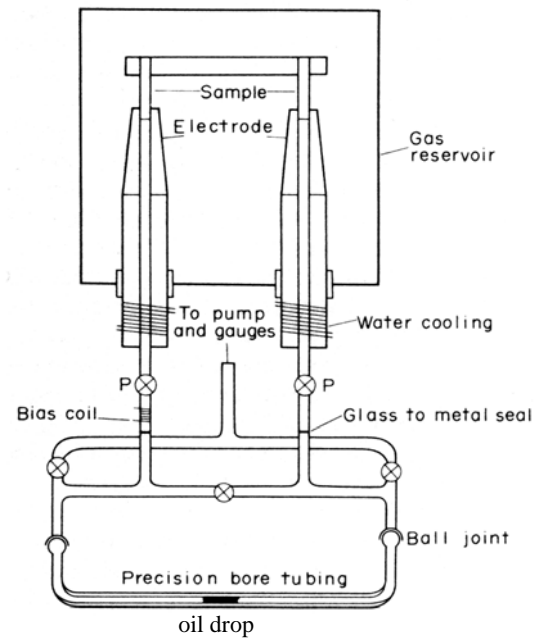


Fig. VIII.14: Schematic (top) drawing of the apparatus used by Einziger and Huntington (1974) to study the electromigration of H in Ag. The drop is promonaphtalene with a low vapor pressure. Detail (bottom) of the hollow electrodes. Gold is used in order to prevent diffusion in the stainless stell 304.

E2 Internal flow measurements

Peterson and Jensen (1977) have proposed to follow the displacement of H by means of the resistive method illustrated in Fig.VIII.15. The two electrodes are placed far enough from the region of large concentration gradient. The time dependence of the resistivity of the sample section A-B is a direct measure of the displacement of the interface as the specific electrical resistivity of the hydride is higher than that of the pure metal.

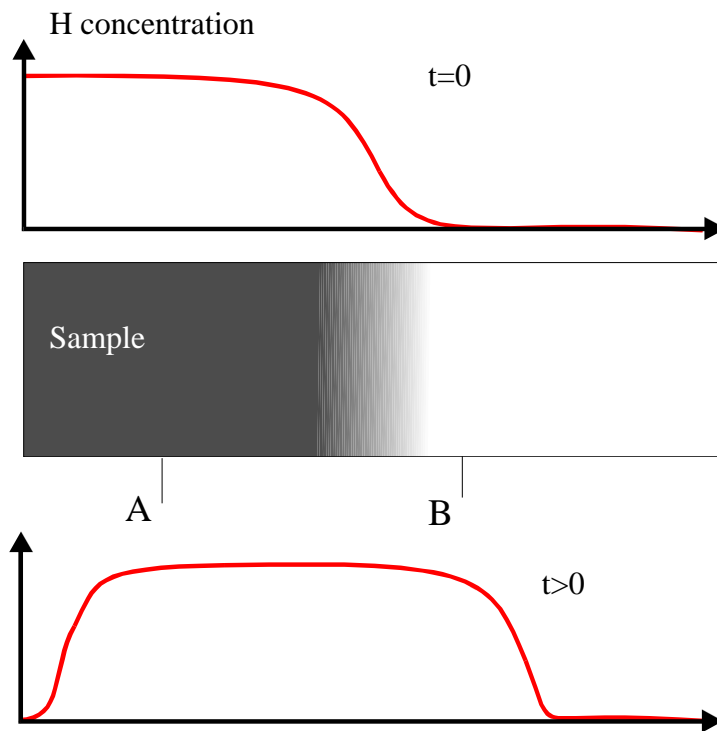


Fig. VIII.15: Method of Peterson and Jensen(1977). The sample is loaded electrolytically in such a way that there is a rather sharp interface in concentration at $t=0$. A high DC current displaces the hydrogen towards one end of the sample. A and B indicate the position of the electrodes used to measure the resistivity of the section A-B.

E3 Concentration gradient measurements

This method is the same as that described in Section D4. In the framework of the thermodynamics of irreversible processes we shall derive the following expression for the steady state concentration gradient dc/dx induced by the electrical potential gradient $d\phi/dx$

$$\frac{dc}{dx} = eZ^* \left(\frac{\partial \mu}{\partial c} \right)^{-1} \frac{d\phi}{dx} \quad (\text{VIII.79})$$

By measuring locally the resistivity at several points on the sample one can derive dc/dx . $\partial \mu / \partial c$ may be evaluated from pressure-composition experiments or from theoretical calculations (see chapter II). This method has been used by Erckman and Wipf (1976) for Nb-H, V-H and Ta-H. More recently, it has been applied by Brouwer et al. to study the diffusion of H in strained vanadium. Experimental data for a $\text{VH}_{0.0097}$ sample at 312 K are shown in Fig.VIII.16.

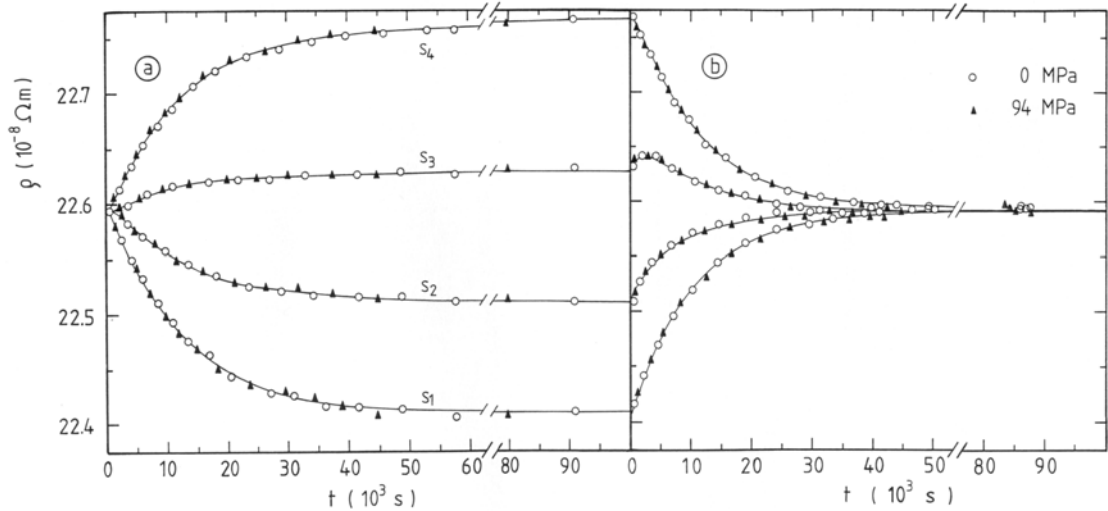


Fig. VIII.16: Time dependence of the electrical resistivity measured on four sections of a $VH_{0.0097}$ sample at 312 K: a) in presence of an electrical current of 384 A/cm^2 and b) after the current has been reduced to zero. Note the momentary increase in hydrogen concentration in section 3 just after the current has been cut off. This is in agreement with the calculated concentration profiles shown in Fig.IV.14.

E4 Dilatometric methods

These methods exploit the fact that hydrogen produces a lattice expansion of the host metal lattice. By measuring the local lattice deformation one can determine the local concentration and map out the concentration profile. For most transition metal hydrides

$$\frac{\Delta l}{l} \cong 5 \cdot 10^{-4} \cdot \left[\frac{H}{M} \right] \quad (\text{VIII.80})$$

These length changes can be easily detected by means of capacitance dilatometric techniques or by X-ray scattering with narrow beams (e.g. $30 \mu\text{m}$ in diameter at the European Synchrotron Research Facility in Grenoble). The advantage of the dilatometric method is that the dilation varies often linearly with the hydrogen concentration in sharp contrast with the electrical resistivity which may depend in a rather complicated way on x in MH_x .

E5 Optical methods

The switchable mirrors are well suited for optical investigations of electromigration since their optical appearance depends in a characteristic way on the local hydrogen concentration. A nice example is shown in Fig.VIII.17 for an yttrium film which is simultaneously loaded with hydrogen from the left and the right through Pd pads. In absence of an electrical current (top panel) the diffusion pattern is symmetric. In the presence of a current a clear asymmetry is

induced (middle panel). The asymmetry can be increased by increasing the current (lower panel). These experiments show unambiguously that Z^* is negative in YH_x .

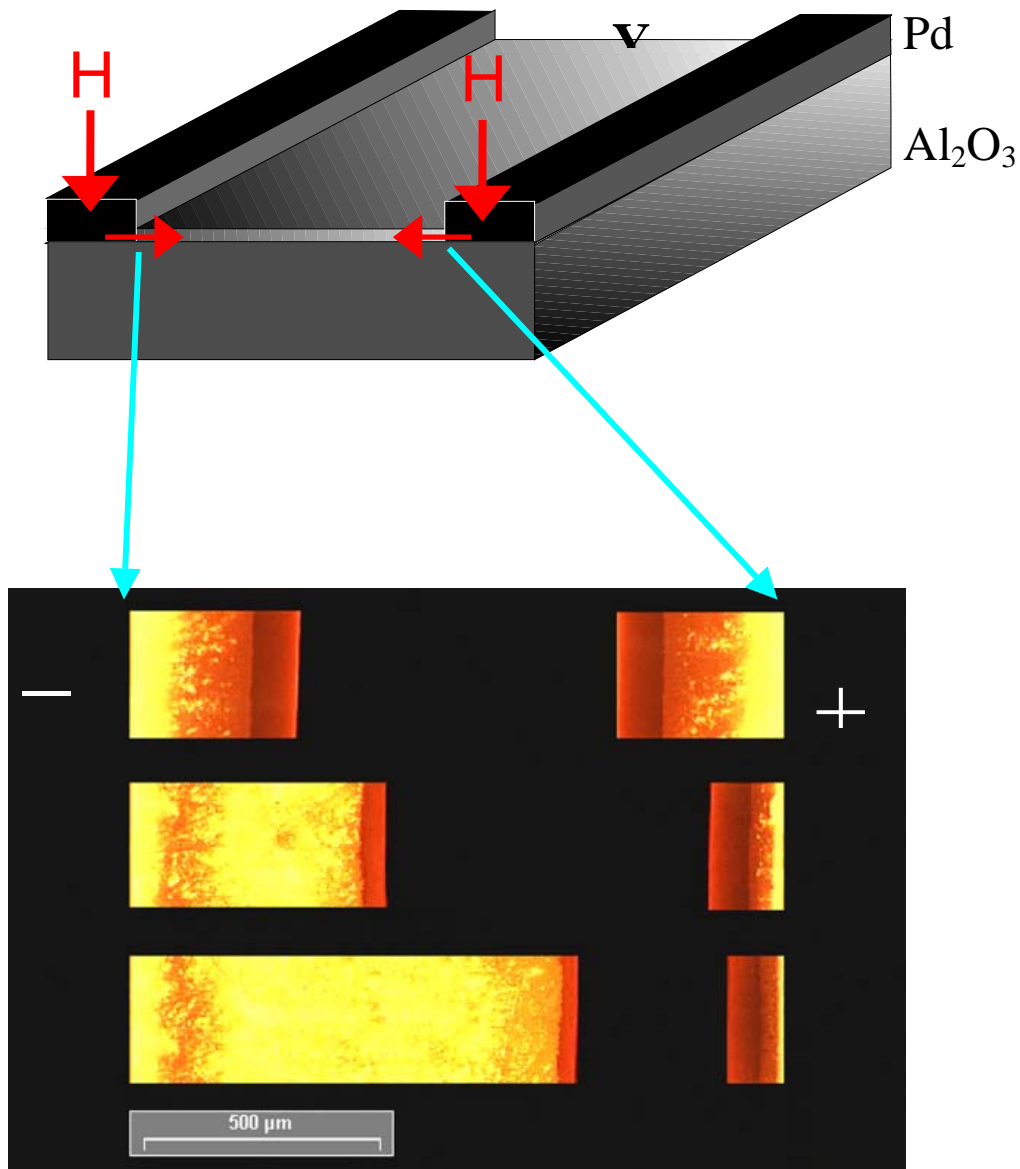


Fig. VIII.17: Electromigration of hydrogen in a 200 nm thick yttrium film at room temperature. As shown in the top figure the yttrium film is covered on both ends with a Pd pad through which hydrogen can be introduced into the film. The photographs are obtained by illuminating the film from the back. Three different situations are investigated: i) in absence of electric current hydrogen penetrates symmetrically into the film, ii) in presence of a current (20 mA) a clear asymmetry is observed as hydrogen is attracted by the positive electrode (on the right in the figure), iii) the asymmetry is even stronger when the current is increased to 40 mA (lower photograph). (van der Molen et al (1998) and den Broeder et al. 1998).

Some experimental data, obtained by means of the methods described before, are given in Table VIII.1 and in Fig.VIII.18. Table VIII.1 shows that in most of the transition metals hydrogen is behaving as a positively charged ion, while for elements at the beginning

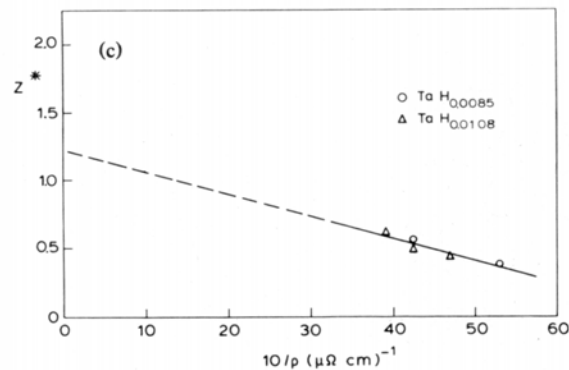
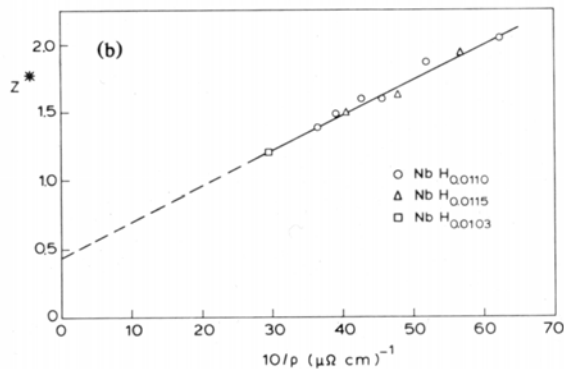
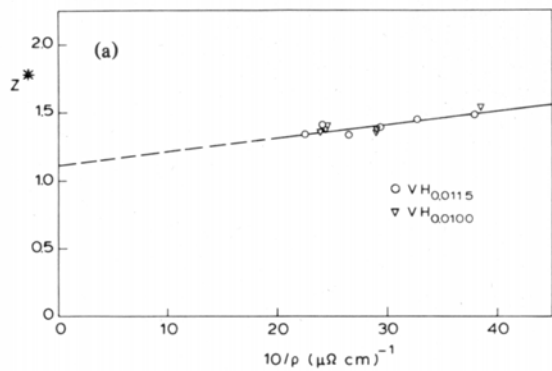
Table VIII.1: Effective charge number Z^* of hydrogen in various metals as determined from electromigration experiments. In most cases the hydrogen concentration is small. An exception is YH_x where x can be as high as 3.

Metal	Z^*	T[K]	Reference
Y	-1	350	van der Molen et al. (1999)
	-1	1025	Carlson et al.(1966)
V	1.54-1.33	276-527	Verbruggen et al. (1986)
Nb	2.04-1.30	276-522	Verbruggen et al. (1986)
Ta	0.38-0.61	377-518	Verbruggen et al. (1986)
Mo	0.29-1.05	289-767	
Fe			
Ni			
Pd	0.80	373	Pietrzak (1991)
Ag			
Cu	-20		

VIII.2 THERMOMIGRATION

The methods used in studies of thermomigration are very similar to those described above for diffusion and electromigration. In thermomigration a concentration gradient in the distribution of hydrogen is produced by a temperature gradient. One defines the heat of transport Q^* in such a way that

$$\frac{d\rho}{dx} = -\frac{Q^*}{\frac{\partial\mu}{\partial\rho} T} \frac{dT}{dx} \quad (\text{VIII.81})$$



and at the end of a series (4d) it behaves in the same way as a negative ion. This point illustrates the complexity of the problem of electromigration. Fig. IV.18 shows the data of Verbruggen et al. for the effective charge number of hydrogen in the group VA metal. The data are plotted as a function of the inverse resistivity ρ as one expects theoretically that

$$Z^* = Z_d + \frac{K}{\rho} \quad (\text{VIII.82})$$

The positive intercept obtained by linear extrapolation to infinite resistivity has been interpreted as an evidence for the existence of a finite **direct force valence** of H in these metals.

Fig. VIII.18: Dependence on electrical resistivity of the effective valence Z^* of hydrogen in V, Nb and Ta determined from electromigration experiments as a function of temperature. The change in resistivity occurs because of electron-phonon scattering. The high temperature data correspond to the points on the left since ρ is highest there.

In Table VIII.2 we give the heat of transport of hydrogen in several metals. Until now thermomigration has received much less theoretical attention than diffusion and electromigration. In the following section we shall apply the thermodynamics of irreversible processes to the transport phenomena discussed previously.

Table VIII.2: Heat of transport of hydrogen in various metals as determined from thermomigration experiments. In most cases the hydrogen concentration is small.

Metal	Q^* [eV]	T [K]	Reference
V	0.017	300	Heller and Wipf (1976)
Nb	0.12	300	Wipf and Alefeld (1974)
Fe	-0.25	850	Gonzalès and Oriani (1965)
Ni	-0.036	850	Gonzalès and Oriani (1965)
Pd	0.065	750	Oates and Shaw (1970)

VIII.3 THERMODYNAMICS OF IRREVERSIBLE PROCESSES

From the experimental methods described so far to measure diffusion, electromigration and thermomigration, we have seen that a migration of particles can be induced by a concentration, an electrical potential or a temperature gradient. Furthermore, especially in the case of electromigration one is dealing with more than one type of particles (charged impurities: H^+ , D^+ , O^{2-} , ... and conduction electrons). In general, one can say that particle currents J_i are produced by forces (the gradient of T , ϕ_k , etc.) X_k and write, in the spirit of linear response theory, that

$$J_i = \sum_{k=1}^n L_{ik} X_k \quad 1 \leq i \leq n \quad (\text{VIII.83})$$

The L_{ik} are sometimes called the phenomenological coefficients (see for example S.R. de Groot 1960). Onsager showed, if the currents J_i and the forces X_k are chosen in an *appropriate way* that the matrix of the phenomenological coefficients L_{ik} is symmetric, i.e.

$$L_{ik} = L_{ki} \quad (\text{VIII.84})$$

In presence of a magnetic field \mathbf{B} this is generalized to

$$L_{ik}(\mathbf{B}) = L_{ki}(-\mathbf{B}) \quad (\text{VIII.85})$$

which implies in particular that

$$L_{ii}(\mathbf{B}) = L_{ii}(-\mathbf{B}), \text{ i.e.} \quad (\text{VIII.86})$$

$$L_{ii} = L_{ii}(B^2) \quad (\text{VIII.87})$$

We have now to define what is meant by an *appropriate way*. For this, let us consider a volume element Ω of a system which is *not* in thermodynamical equilibrium. The variation of the entropy dS/dt of this volume element is made up of two contributions dS_{ext}/dt and dS_{int}/dt , so that

$$\frac{dS}{dt} = \frac{dS_{\text{ext}}}{dt} + \frac{dS_{\text{int}}}{dt} \quad (\text{VIII.88})$$

where dS_{ext} is the entropy supplied by the rest of the system to the element Ω and dS_{int} is the entropy production inside Ω , which is necessary to reach equilibrium. dS_{int} is thus a source of entropy while dS_{ext} is associated with an entropy current. It will be possible, therefore, to write a continuity equation for the entropy density in the following form

$$\frac{\partial s}{\partial t} + \text{div} \mathbf{J}_s = \sigma \quad (\text{VIII.89})$$

where $s=S/\Omega$

$$\frac{dS_{ext}}{dt} = - \int_{opp(\Omega)} \mathbf{J}_s \cdot d\mathbf{Q} \quad (\text{VIII.90})$$

and

$$\frac{dS_{int}}{dt} = \int_{\Omega} \sigma dV \quad (\text{VIII.91})$$

where σ is the entropy source density (entropy per cm^3 per sec). With these definitions we can now reformulate Onsager's theorem, more precisely as follows.

If the entropy source σ is given by

$$\sigma = \sum_i J_i X_i \quad (\text{VIII.92})$$

then the matrix L of the coefficient L_{ik} relating the currents J_i to the forces X_k is symmetric.

This theorem is a consequence of the time reversal invariance of the equation of motion of particles. A demonstration may be found in de Groot and Mazur (1962).

From Eq.VIII.92 one can see that the entropy source plays a fundamental role in the thermodynamics of non-equilibrium phenomena and we shall now indicate a way of calculating σ .

The idea is as follows. We postulate that the entropy S of the volume element Ω is a function of

- i) the internal energy U (of the volume element)
- ii) the volume Ω
- iii) the number of particles N_k (k indicates the type of particles: ions, electrons, etc.)

In other words we postulate that

$$T \frac{dS}{dt} = \frac{dU}{dt} + p \frac{d\Omega}{dt} - \sum_{k=1}^n \mu_k \frac{dN_k}{dt} \quad (\text{VIII.93})$$

for an observator moving with the centre of gravity of the volume element. The symbol d/dt is the *substantial derivative* which is related to the local time derivative $\partial/\partial t$ by means of the following relation

$$\frac{d \cdot}{dt} = \frac{\partial \cdot}{\partial t} + \mathbf{v} \text{grad} \cdot \quad (\text{VIII.94})$$

where \mathbf{v} is the velocity of the center of gravity. We are now going to evaluate dU/dt and dN_k/dt in order to find dS/dt . Then by means of Eq.VIII.94 we will obtain a relation of the form of the continuity equation (see Eq.VIII.89) to identify an entropy source term and a divergence of a current term. All these steps are necessary because the first law of thermodynamics cannot be used for our volume element in the form

$$\frac{dU}{dt} = \frac{dQ^\downarrow}{dt} - p \frac{d\Omega}{dt} + \sum_k \mu_k \frac{dN_k}{dt} \quad (\text{VIII.95})$$

because Ω is in contact with the rest of the system. As an example consider the case where a heat dQ^\downarrow is given to the volume element. $dU \neq dQ^\downarrow$ because of heat conduction out of Ω . What we need is thus a reformulation of the first law for our volume element.

For this we are going to use the following laws of conservation and equation of motion:

I. Conservation of the number of particles of type k. We do not allow for chemical reactions

$$\frac{\partial \left(\frac{N_k}{\Omega} \right)}{\partial t} + \text{div} \left(\frac{N_k}{\Omega} \mathbf{v}_k \right) = 0 \quad (\text{VIII.96})$$

II. Conservation of the total energy: $E = E_{\text{kin}} + E_{\text{pot}} + U$

$$\frac{\partial \left(\frac{E}{\Omega} \right)}{\partial t} + \text{div} \mathbf{J}_e = 0 \quad (\text{VIII.97})$$

III. The equation of motion of the centre of gravity of the volume element

$$m \frac{d\mathbf{v}}{dt} = \sum_k \mathbf{f}_k \frac{N_k}{\Omega} - \text{grad} p \quad (\text{VIII.98})$$

with

$$m = \frac{\sum_k N_k m_k}{\Omega} \quad (\text{VIII.99})$$

where m_k is the mass of one particle of type k, and \mathbf{f}_k is the force on one particle of type k which is equal to $-\text{grad} \phi_k$ (where ϕ_k is the potential) and p is the pressure.

To make contact with Eq.VIII.97 let us calculate $\partial e_{kin}/\partial t$ (e_{kin} is equal to E_{kin}/Ω)

$$\begin{aligned}
\frac{\partial(\frac{1}{2}mv^2)}{\partial t} &\stackrel{Eq.VIII.94}{=} \frac{d(\frac{1}{2}mv^2)}{dt} - \mathbf{v} \cdot \text{grad}(\frac{1}{2}mv^2) \\
&= m\mathbf{v} \cdot \frac{d\mathbf{v}}{dt} + \frac{1}{2}v^2 \frac{dm}{dt} - \mathbf{v} \cdot \text{grad}(\frac{1}{2}mv^2) \\
&= \sum_k \mathbf{v} \cdot \mathbf{f}_k n_k - \mathbf{v} \cdot \text{grad}p + \frac{1}{2}v^2 \left[\frac{\partial m}{\partial t} + \mathbf{v} \text{grad}m \right] \\
&\quad - \mathbf{v} \cdot \text{grad}(\frac{1}{2}mv^2)
\end{aligned} \tag{VIII.100}$$

From the conservation of the total number of particles follows that

$$\frac{\partial m}{\partial t} + \text{div} m\mathbf{v} = 0 \tag{VIII.101}$$

and noting that

$$\text{div}(\frac{1}{2}mv^2)\mathbf{v} = (\frac{1}{2}v^2)\text{div} m\mathbf{v} + m\mathbf{v} \cdot \text{grad}(\frac{1}{2}v^2) \tag{VIII.102}$$

we obtain finally

$$\frac{\partial e_{kin}}{\partial t} = -\text{div}[(\frac{1}{2}mv^2)\mathbf{v}] - \mathbf{v} \cdot \text{grad}p + \sum \mathbf{v} \cdot \mathbf{f}_k n_k \tag{VIII.103}$$

since $\mathbf{v}p$ is an energy current density (due to the mechanical work performed by the pressure) one can rewrite Eq.VIII.103 in the form

$$\frac{\partial e_{kin}}{\partial t} = -\text{div}[(\frac{1}{2}mv^2)\mathbf{v} + \mathbf{v}p] - p\text{div} \mathbf{v} + \sum \mathbf{v} \cdot \mathbf{f}_k n_k \tag{VIII.104}$$

Let us now evaluate the potential energy contribution to Eq.VIII.97, $\partial e_{kin}/\partial t$,

$$\frac{\partial e_{pot}}{\partial t} = \frac{\partial \left(\sum_k N_k \varphi_k / \Omega \right)}{\partial t} = \frac{\partial}{\partial t} \sum_k n_k \varphi_k = \sum_k \varphi_k \frac{\partial n_k}{\partial t} \tag{VIII.105}$$

The last equation follows from the assumption that the forces \mathbf{f}_k and thus the potentials φ_k do not depend on time. From the continuity equation Eq.VIII.96, we have

$$\frac{\partial e_{pot}}{\partial t} = -\sum_k \varphi_k \operatorname{div} \mathbf{v}_k n_k \quad (\text{VIII.106})$$

As we want, eventually, to calculate dS/dt , i.e. a quantity seen by an observer moving with the centre of gravity of the volume element, it is now meaningful to define currents of particles for a reference frame attached to the centre of gravity of Ω . Doing this by the following relation

$$\mathbf{J}_k = n_k (\mathbf{v}_k - \mathbf{v}) \quad (\text{VIII.107})$$

we rewrite Eq.VIII.106 as follows,

$$\frac{\partial e_{pot}}{\partial t} = -\sum_k \varphi_k \operatorname{div} \mathbf{J}_k - \sum_k \varphi_k \operatorname{div} n_k \mathbf{v} \quad (\text{VIII.108})$$

The potential energy density is $\sum_k n_k \varphi_k$. The corresponding convective-potential-energy-current-density is $\mathbf{v} \sum_k n_k \varphi_k$. This is why we write

$$\begin{aligned} \sum_k \varphi_k \operatorname{div} n_k \mathbf{v} &= \operatorname{div} \left(\sum_k \varphi_k n_k \mathbf{v} \right) - \sum_k n_k \mathbf{v} \cdot \operatorname{grad} \varphi_k \\ &= \operatorname{div} \left(\sum_k \varphi_k n_k \mathbf{v} \right) - \sum_k n_k \mathbf{v} \cdot \mathbf{f}_k \end{aligned} \quad (\text{VIII.109})$$

Similarly, as $\varphi_k \mathbf{J}_k$ represent also a potential-energy-current-density, we write,

$$\begin{aligned} \sum_k \varphi_k \operatorname{div} \mathbf{J}_k &= \operatorname{div} \left(\sum_k \varphi_k \mathbf{J}_k \right) - \sum_k \mathbf{J}_k \cdot \operatorname{grad} \varphi_k \\ &= \operatorname{div} \left(\sum_k \varphi_k \mathbf{J}_k \right) - \sum_k \mathbf{J}_k \cdot \mathbf{f}_k \end{aligned} \quad (\text{VIII.110})$$

For the sum of potential and kinetic energy we have from Eqs.VIII.104, 108 and 110,

$$\begin{aligned} \frac{\partial (e_{kin} + e_{pot})}{\partial t} &= -\operatorname{div} \left((e_{kin} + e_{pot}) \mathbf{v} + \mathbf{v} p + \sum_k \varphi_k \mathbf{J}_k \right) \\ &\quad + p \operatorname{div} \mathbf{v} - \sum_k \mathbf{J}_k \cdot \mathbf{f}_k \end{aligned} \quad (\text{VIII.111})$$

or introducing a mechanical-energy-current-density \mathbf{J}_M

$$\mathbf{J}_M = (e_{kin} + e_{pot}) \mathbf{v} + \mathbf{v} p + \sum_k \varphi_k \mathbf{J}_k \quad (\text{VIII.112})$$

and a mechanical-energy-density-source σ_M

$$\frac{\partial(e_{kin} + e_{pot})}{\partial t} + \text{div}\mathbf{J}_M = \sigma_M \quad (\text{VIII.113})$$

The sum of kinetic and potential energy is not conserved, only the total energy! (see Eq.VIII.97). \mathbf{J}_M does not include any heat flow and we define now a heat-current-density \mathbf{J}_Q in such a way that

$$\mathbf{J}_e \equiv \mathbf{J}_M + \mathbf{J}_Q + U\mathbf{v} \quad (\text{VIII.114})$$

We obtain then from Eqs.VIII.109 and 112 a continuity equation for the internal energy density U ,

$$\frac{\partial u}{\partial t} + \text{div}(u\mathbf{v} + \mathbf{J}_Q) = -p\text{div}\mathbf{v} + \sum_k \mathbf{J}_k \cdot \mathbf{f}_k \quad (\text{VIII.115})$$

Using the relation between d/dt and $\partial/\partial t$ (Eq.VIII.94) we have

$$\begin{aligned} \frac{du}{dt} &= -\text{div}(u\mathbf{v} + \mathbf{J}_Q) - p\text{div}\mathbf{v} + \sum_k \mathbf{J}_k \cdot \mathbf{f}_k + \mathbf{v} \cdot \text{grad}u \\ &= -\text{div}\mathbf{J}_Q - u\text{div}\mathbf{v} - p\text{div}\mathbf{v} + \sum_k \mathbf{J}_k \cdot \mathbf{f}_k \end{aligned} \quad (\text{VIII.116})$$

Noting that $\text{div}\mathbf{v} = \frac{d\Omega}{\Omega dt}$ we find that

$$\begin{aligned} \frac{dU}{dt} &= \frac{d(u\Omega)}{dt} = u \frac{d\Omega}{dt} + \Omega \frac{du}{dt} \\ &= u \frac{d\Omega}{dt} - \Omega \text{div}\mathbf{J}_Q - \Omega u \text{div}\mathbf{v} - \Omega p \text{div}\mathbf{v} + \Omega \sum_k \mathbf{J}_k \cdot \mathbf{f}_k \\ &= -\Omega \text{div}\mathbf{J}_Q - p \frac{d\Omega}{dt} + \Omega \sum_k \mathbf{J}_k \cdot \mathbf{f}_k \end{aligned} \quad (\text{VIII.117})$$

and by inserting this result into Eq.VIII.93 we obtain the following expression for the entropy change

$$T \frac{dS}{dt} = -\Omega \text{div}\mathbf{J}_Q + \Omega \sum_k \mathbf{J}_k \cdot \mathbf{f}_k - \sum_k \mu_k \frac{dN_k}{dt} \quad (\text{VIII.118})$$

The last step is now to express dN_k/dt in terms of the particle-current-densities \mathbf{J}_k . From Eq.VIII.93 and 95 we obtain

$$\frac{\partial n_k}{\partial t} + \text{div} n_k \mathbf{v}_k = 0 \quad (\text{VIII.119})$$

$$\begin{aligned} \frac{\partial n_k}{\partial t} + \text{div}(\mathbf{J}_k + n_k \mathbf{v}) &= \frac{\partial n_k}{\partial t} + \text{div} \mathbf{J}_k + n_k \text{div} \mathbf{v} + \mathbf{v} \cdot \text{grad} n_k \\ &= \frac{dn_k}{dt} + \text{div} \mathbf{J}_k + n_k \frac{1}{\Omega} \frac{d\Omega}{dt} = 0 \end{aligned} \quad (\text{VIII.120})$$

or equivalently

$$\frac{d(\Omega n_k)}{dt} = -\Omega \text{div} \mathbf{J}_k = \frac{dN_k}{dt} \quad (\text{VIII.121})$$

We have thus

$$\frac{dS}{dt} = -\frac{\Omega}{T} \text{div} \mathbf{J}_\rho + \frac{\Omega}{T} \sum_k \mathbf{J}_k \cdot \mathbf{f}_k + \frac{\Omega}{T} \sum_k \mu_k \text{div} \mathbf{J}_k \quad (\text{VIII.122})$$

For a unit volume element

$$\frac{d(S/\Omega)}{dt} = -\frac{1}{T} \text{div} \mathbf{J}_\rho + \frac{1}{T} \sum_k \mathbf{J}_k \cdot \mathbf{f}_k + \frac{1}{T} \sum_k \mu_k \text{div} \mathbf{J}_k - \frac{S}{\Omega^2} \frac{d\Omega}{dt} \quad (\text{VIII.123})$$

We want now to cast this expression in the form of the equation of continuity for the entropy (see Eq.VIII.89)

$$\begin{aligned} \frac{dS}{dt} &= -\text{div} \left(\frac{\mathbf{J}_\rho}{T} \right) + \mathbf{J}_\rho \cdot \text{grad} \frac{1}{T} - \sum_k \mathbf{J}_k \cdot \text{grad} \frac{\mu_k}{T} + \text{div} \left(\sum_k \frac{\mu_k \mathbf{J}_k}{T} \right) \\ &\quad + \frac{1}{T} \sum_k \mathbf{J}_k \cdot \mathbf{f}_k - S \text{div} \mathbf{v} \end{aligned} \quad (\text{VIII.124})$$

However,

$$\frac{dS}{dt} = \frac{\partial \mathcal{S}}{\partial t} + \mathbf{v} \cdot \text{grad} s = \frac{\partial \mathcal{S}}{\partial t} + \text{div}(s\mathbf{v}) - s \text{div} \mathbf{v} \quad (\text{VIII.125})$$

Thus

$$\frac{\partial \mathcal{S}}{\partial t} + \text{div} \left[\frac{\mathbf{J}_Q}{T} - \sum_k \frac{\mu_k \mathbf{J}_k}{T} - \mathbf{v} s \right] = \frac{1}{T} \sum_k \mathbf{J}_k \cdot \left[\mathbf{f}_k - T \text{grad} \frac{\mu_k}{T} \right] + \mathbf{J}_Q \cdot \text{grad} \frac{1}{T} \quad (\text{VIII.126})$$

The entropy source is thus

$$\sigma = \mathbf{J}_Q \cdot \text{grad} \frac{1}{T} + \sum_k \mathbf{J}_k \cdot \left[\mathbf{f}_k - T \text{grad} \frac{\mu_k}{T} \right] \quad (\text{VIII.127})$$

and by comparison with Eq.VIII.98 we have

$$\begin{aligned} \mathbf{X}_Q &= \text{grad} \frac{1}{T} \\ \mathbf{X}_k &= \frac{\mathbf{f}_k}{T} - \text{grad} \left(\frac{\mu_k}{T} \right) \end{aligned} \quad (\text{VIII.128})$$

Very often mechanical equilibrium is reached much faster than thermodynamical equilibrium. To good approximation one can assume that $d\mathbf{v}/dt=0$ in Eq.IV.92 and thus

$$\text{grad} p = \sum_k \mathbf{f}_k n_k \quad (\text{VIII.129})$$

This relation assumes a particularly simple form in the case of isothermal processes, where $\text{grad} T=0$. Then

$$\mathbf{X}_Q = 0 \quad (\text{VIII.130})$$

and

$$\mathbf{X}_k = \frac{1}{T} (\mathbf{f}_k - \text{grad} \mu_k) \quad (\text{VIII.131})$$

We shall show now that Eq.VIII.129 implies that

$$\sum_k n_k \mathbf{X}_k = 0 \quad (\text{VIII.132})$$

for isothermal processes in mechanical equilibrium. For the proof we just have to remember that

$$G = \sum_k \mu_k N_k \quad (\text{VIII.133})$$

and

$$G = U - TS + pV \quad (\text{VIII.134})$$

For an isothermal process

$$dG = \Omega dp + \sum_k \mu_k dN_k = \sum_k \mu_k dN_k + \sum_k N_k d\mu_k \quad (\text{VIII.135})$$

Thus

$$\Omega dp = \sum_k N_k d\mu_k \quad (\text{VIII.136})$$

or

$$grad p = \sum_k n_k grad \mu_k \quad (\text{VIII.137})$$

Introducing this relation into Eq.VIII.129 we obtain

$$\sum_k n_k (\vec{f}_k - grad \mu_k) = 0 \quad (\text{VIII.138})$$

We have now all the ingredients to discuss diffusion, electromigration and thermomigration of interstitials (such as H, D, T, C, O, N, B) in metals.

VIII.3.1 DIFFUSION

We have just one component and no external forces. Thus as T=const.

$$\mathbf{X}_d = -\frac{1}{T} grad \mu_H \quad (\text{VIII.139})$$

and

$$\mathbf{J}_d = L_d \mathbf{X}_d = -\frac{L_d}{T} grad \mu_H \quad (\text{VIII.140})$$

Fick's first law is, however, given in terms of a concentration gradient,

$$\mathbf{J}_d = -D \text{grad} \rho_H \quad \rho_H = \frac{N_H}{\Omega} = \text{number of } H \text{ per unit volume} \quad (\text{VIII.141})$$

Thus

$$D = \frac{L}{T} \frac{\partial \mu}{\partial \rho_H} \Big|_T \quad (\text{VIII.142})$$

Using the same notation as previously

$$\frac{TD}{L_d} = \frac{1}{K\rho^2} \quad (\text{VIII.143})$$

and thus, on a line of constant concentrations $c_H = c_{\text{critical}}$ we obtain that

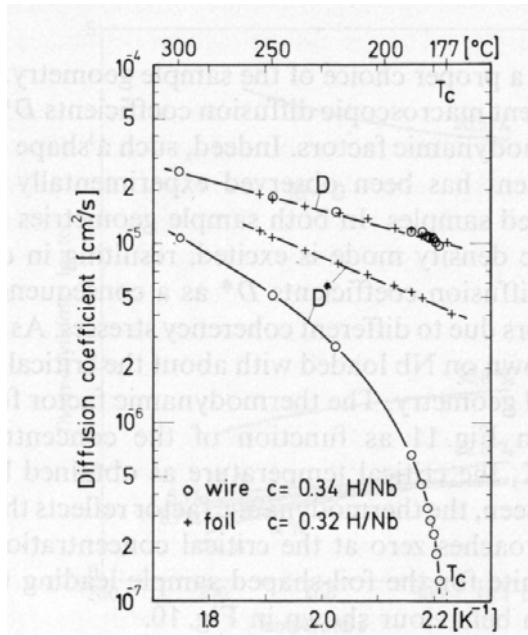


Fig. VIII.19: Macroscopic diffusion coefficient and tracer diffusion coefficient for H in a Nb wire and a Nb foil. For concentrations close to the critical concentration ($c=0.34$) D tends to zero and we have a regime of critical slowing down. Note that the so-called tracer diffusion coefficient measured by means of neutron scattering does not suffer from critical slowing down. As a result of the long range elastic interaction the macroscopic diffusion coefficient is influenced by the shape of the sample (see Fig.II.37).

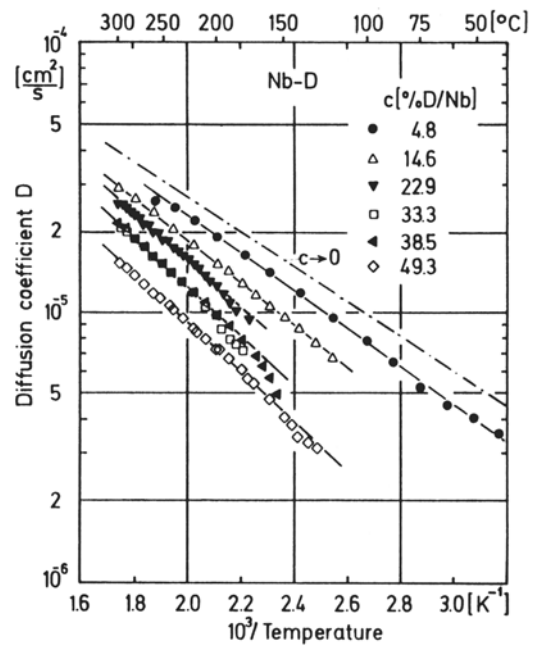


Fig. VIII.20: Concentration dependence of the tracer diffusion coefficient for deuterium (D) in Nb. The tracer diffusion coefficient does not depend on the thermodynamic factor (the concentration dependence of the chemical potential in Eq.IV.134. Völkl and Alefeld (1979).

$$D = \frac{L_d}{T} k(T - T_c) \frac{\rho_{mi}}{\rho_{crit}^2} \quad (\text{VIII.144})$$

Such a behaviour (critical slowing down) is nicely shown in Fig.VIII.19 for the diffusion of H in Nb.

In the limit of low concentrations, we have

$$\lim_{c_H \rightarrow 0} \frac{\partial \mu_H}{\partial c_H} = \frac{kT}{c_H} \rightarrow \frac{\partial \mu_H}{\partial \rho_H} = \frac{kT}{\rho_H} \quad (\text{VIII.145})$$

and thus

$$D = \frac{L_d}{T} \frac{kT}{\rho_H} = \frac{kL_d}{\rho_H} \quad (\text{VIII.146})$$

This shows that $L_d \sim \rho_H$ in order to have a finite diffusion constant at a low concentration. This reminds us that the L_{ik} parameters in Eq.VIII.81 are just phenomenological parameters which may depend on T , ρ , p , ... but not on the external force or gradient of thermodynamical quantities. The concentration dependence of D for H in Nb is shown in Fig.VIII.20. A review on the microscopic theory for the diffusion of hydrogen in metals may be found in the book by Fukai (1993).

VIII.3.2 ELECTROMIGRATION

Until now we have always considered currents in the centre of gravity reference frame. In electromigration it is more natural to attach the frame of reference to the host metal lattice. As shown by Prigogine, the expression for the entropy production remains the same in the two lattices. This follows directly from the fact that

$$\sum_n n_k \mathbf{X}_k = 0 \quad (\text{VIII.147})$$

In the centre of gravity we have defined particle current densities

$$\mathbf{J}_k = n_k (\mathbf{v}_k - \mathbf{v}) \quad (\text{VIII.148})$$

Let us define new fluxes

$$\mathbf{J}_k' = n_k (\mathbf{v}_k - \mathbf{v}') \quad (\text{VIII.149})$$

And calculate

$$\sigma' T = \sum_k \mathbf{J}_k' \cdot \mathbf{X}_k = \sum_k \mathbf{J}_k \cdot \mathbf{X}_k + \sum_k n_k (\mathbf{v} - \mathbf{v}') \cdot \mathbf{X}_k = \sum_k \mathbf{J}_k \cdot \mathbf{X}_k \quad (\text{VIII.150})$$

The last equality in Eq.VIII.150 follows directly from of Eq.VIII.132. This implies that in the frame of reference attached to the lattice Onsager's theorem is also valid and we can write the following relation for the electron currents \mathbf{J}_e' and migrating interstitials \mathbf{J}_i ,

$$\begin{aligned} \mathbf{J}_e' &= \frac{L_{ee}'}{T} Z_e |e| \mathbf{E} + \frac{L_{ei}'}{T} Z_i |e| \mathbf{E} \\ \mathbf{J}_i' &= \frac{L_{ie}'}{T} Z_e |e| \mathbf{E} + \frac{L_{ii}'}{T} Z_i |e| \mathbf{E} \end{aligned} \quad (\text{VIII.151})$$

for a situation without gradients in chemical potentials.. Z_i is the charge of the unscreened ion and $Z_e = -1$ for the electron. Thus

$$\mathbf{J}_i' = \frac{L_{ee}'}{T} \left(Z_e |e| - \frac{L_{ie}'}{L_{ii}'} |e| \right) \mathbf{E} \quad (\text{VIII.152})$$

and the effective charge number Z^* of the migrating ion is

$$Z^* = Z_i - \frac{L_{ie}'}{L_{ii}'} \quad (\text{VIII.153})$$

and the total force acting on the ion is

$$\mathbf{F} = |e| Z^* \vec{\mathbf{E}} = \underbrace{|e| Z_i \mathbf{E}}_{\text{direct force}} - \underbrace{\frac{L_{ie}'}{L_{ii}'} |e| \mathbf{E}}_{\text{electron wind force}} \quad (\text{VIII.154})$$

The existence of a direct force has been a very controversial matter until 1990. We believe that the articles of Das (1976), Das and Peierls (1973) and Sorbello (1977) has unambiguously demonstrated that the direct force exists.

There are however still theorists in favor of a zero direct force (see Bosvieux and Friedel (1962)), Gerl (1971), Turban et al (1976) and Hesketh (1978). They would argue here that $Z_i = 0$ because the migrating ion is completely shielded. There are however some experimental evidences that $Z_i \neq 0$. For this, let us go back to Fig.IV.16 which shows that at low temperatures Z^* assumes values between 0.5 and 3.5 for the VA metals, while at high temperatures the values

are within 0.8 and 1.6. How can we understand this convergence of the Z^* values at high temperatures?

Let us assume that hydrogen migrates under the influence of the electric field by hopping from one interstitial site to another. Such a hopping migration is strongly facilitated by high temperatures as is seen in the temperature variation of the diffusion coefficient. One expects thus L_{II}' increases with temperature (if we had neglected the non-diagonal terms $L_{Ie}'=L_{eI}'=0$, then we would have $L_{II}'=D\rho_H/k$). On the other hand L_{eI}' is expected to decrease with increasing temperature, as the electrical conductivity of a metal does. This means then that at high temperatures the electron wind term may be neglected and we have just the direct force term. With this interpretation in mind, the data shown in Fig.VIII.18 would imply that the charge of the unscreened hydrogen ion is essentially one (as expected for a proton).

Before leaving the phenomenological theory of electromigration, let us just make a comment regarding Eq.VIII.72, where we have treated the migration of an interstitial as a one component system, the migrating ions, and wrote essentially

$$\mathbf{J}_i' = \frac{L_i'}{T} (eZ_i^* \mathbf{E} - \text{grad}\mu_i) \quad (\text{VIII.155})$$

More correctly we should have written

$$\begin{aligned} \mathbf{J}_e' &= -\frac{L_{ee}'}{T} |e| \mathbf{E} + \frac{L_{ei}'}{T} (Z_i |e| \mathbf{E} - \text{grad}\mu_i) \\ \mathbf{J}_i' &= -\frac{L_{ei}'}{T} |e| \mathbf{E} + \frac{L_{ii}'}{T} (Z_i |e| \mathbf{E} - \text{grad}\mu_i) \end{aligned} \quad (\text{VIII.156})$$

We have neglected $\text{grad}\mu_e \cong \text{grad}E_F = 0$ as in a metal a gradient in Fermi energy would lead to huge electrostatic fields. Then

$$\begin{aligned} \mathbf{J}_i' &= \frac{L_{ii}'}{T} \left(Z_i |e| - \frac{L_{ei}'}{L_{ii}'} |e| \right) \mathbf{E} - \frac{L_{ii}'}{T} \text{grad}\mu_i \\ &= \frac{L_{ii}'}{T} Z^* |e| \mathbf{E} - \frac{L_{ii}'}{T} \text{grad}\mu_i \end{aligned} \quad (\text{VIII.157})$$

In agreement with Eq.VIII.155 thus also with Eq.VIII.72.

VIII.3.3 THERMOMIGRATION

In order to derive Eq.VIII.79 let us consider a situation where $\mathbf{f}_k=0$ (no external forces). Then from Eq.VIII.128 we write

$$\mathbf{J}_Q = L_{QQ} \text{grad} \frac{1}{T} + L_{QI} \left(-\text{grad} \left(\frac{\mu_I}{T} \right) \right) \quad (\text{VIII.158})$$

$$\mathbf{J}_I = L_{IQ} \text{grad} \frac{1}{T} + L_{II} \left(-\text{grad} \left(\frac{\mu_I}{T} \right) \right) \quad (\text{VIII.159})$$

We consider now a situation where $\mathbf{J}_Q \neq 0$ but $\mathbf{J}_I = 0$. Then Eq.VIII.158 reduces to

$$\text{grad} \left(\frac{\mu_I}{T} \right) = \frac{L_{IQ}}{L_{II}} \text{grad} \frac{1}{T} \quad (\text{VIII.160})$$

$$\text{grad} \mu_I = \frac{1}{T} \underbrace{\left(\mu_I - \frac{L_{IQ}}{L_{II}} \right)}_{\equiv -Q^*} \text{grad} T \quad (\text{VIII.161})$$

For a one-dimensional system follows then that

$$\frac{d\rho}{dx} \frac{\partial \mu}{\partial \rho} = -\frac{Q^*}{T} \frac{dT}{dx} \quad (\text{VIII.162})$$

which leads to Eq.VIII.79. For small concentrations

$$\frac{d\rho}{dx} = -\frac{Q^* \rho}{kT^2} \frac{dT}{dx} \quad (\text{VIII.163})$$

with

$$Q^* = -kT \ln c_H + \frac{L_{IQ} k}{\rho_H D} \quad (\text{VIII.164})$$

If Q^* remains finite for $c_H \rightarrow 0$ then $L_{IQ} \rightarrow 0$. This follows from Eq.VIII.164 by multiplying by ρ_H and noting that $\rho_H \ln c_H \rightarrow 0$ for $c_H \rightarrow 0$.

VIII.4 REFERENCES